MODELLING VERTICALLY LOADED PILE GROUPS BY CONSIDERING PILE-SOIL-PILE INTERACTIONS

A Thesis Submitted to
the Graduate School of
İzmir Institute of Technology
in Partial Fulfillment of the Requirements for Degree of

MASTER OF SCIENCE

In Civil Engineering

by
Ömer Faruk KAMIŞ

December 2023
İZMİR

We approve the thesis of **Ömer Faruk KAMIŞ**

Examining Committee Members:

Prof. Dr. Alper SEZER
Department of Civil Engineering, Ege University

Doç. Dr. Gürsoy TURAN
Department of Civil Engineering, İzmir Institute of Technology

Asst. Prof. Dr. Volkan İŞBUĞA
Department of Civil Engineering, İzmir Institute of Technology

8 December 2023

Asst. Prof. Dr. Volkan İŞBUĞA
Supervisor, Department of Civil Engineering, İzmir Institute of Technology

Prof. Dr. Cemalettin DÖNMEZ
Head of the Department of Civil Engineering

Prof. Dr. Mehtap EANES
Dean of the Graduate School

ACKNOWLEDGMENTS

I would like to present my deepest gratitude to my thesis advisor Dr. Volkan İşbuğa for his patience and support in the completion of this thesis.

ABSTRACT

MODELLING VERTICALLY LOADED PILE GROUPS BY CONSIDERING PILE-SOIL-PILE INTERACTIONS

The aim of the study presented in this thesis is to create a model that takes into account the interaction between piles for the analysis of pile groups embedded in a linear elastic medium. This research builds upon prior work by Vallabhan and Mustafa (1996) introduced a single pile model and the pile-soil-pile interaction model proposed by İşbuğa (2023). The model has undergone further development to encompass the entire spectrum of pile groups regardless of how many piles it has and what kind of layout it has. This comprehensive model addresses two distinct scenarios: one involving a free-head pile group and another featuring a pile group that has a rigid pile cap.

In the context of a free-head pile group, single piles within the group show different displacements due to load and interactions. On the other hand, in the case of a rigid pile cap, the piles must have equal displacements because of the rigid nature of the pile cap. Two different algorithms have been developed for both of these scenarios, and these algorithms have been implemented using the Python programming language.

The model has been used to analyze various pile groups, and the analysis results were compared with previous studies and finite element method solutions. In addition to comparing the results, the computation times of the models proposed by this study and those of the finite element method were also compared.

ÖZET

KAZIK-ZEMİN-KAZIK ETKİLEŞİMLERİNİ DİKKATE ALARAK DÜŞEY YÜKLÜ KAZIK GRUPLARININ MODELLENMESİ

Bu tezde sunulan çalışmanın amacı, elastik zemin katmanlarına yerleştirilmiş kazık gruplarının analizinde kazıklar arası etkileşimi de hesaba katan bir elastik model oluşturmaktır. Bu araştırma, Vallabhan ve Mustafa (1996) tarafından tek kazıklı bir modelin yanı sıra İşbuğa (2023) tarafından önerilen kazık-zemin-kazık etkileşim modelinin tanıtıldığı önceki çalışmalara dayanmaktadır. Model, kaç kazığa sahip olduğuna ve ne tür bir yerleşime sahip olduğuna bakılmaksızın tüm kazık grupları yelpazesini kapsayacak şekilde daha da geliştirilmiştir. Bu kapsamlı model iki farklı senaryoyu ele almaktadır: biri kazık başlığı bulunmayan durum, diğeri ise rijit bir kazık başlığının olduğu durum.

Kazık başlığı bulunmadığı durumda, grup içindeki münferit kazıklar yük ve etkileşimler nedeniyle farklı yer değiştirmeler gösterebilir. Öte yandan, rijit bir kazık başlığı durumunda, kazık başlığının rijit yapısı nedeniyle kazıkların eşit yer değiştirmelere sahip olması gerekir. Bu senaryoların her ikisi için de iki farklı algoritma geliştirilmiş ve bu algoritmalar Python programlama dili kullanılarak uygulanmıştır.

Model, çeşitli kazık gruplarını analiz etmek için kullanılmış ve analiz sonuçları önceki çalışmalar ve sonlu elemanlar yöntemi çözümleri ile karşılaştırılmıştır. Sonuçların karşılaştırılmasının yanı sıra bu çalışmada yazılan program ile oluşturulan modeller ile sonlu elemanlar yöntemi ile oluşturulan modellerin çözüm hızları da karşılaştırılmıştır.

TABLE OF CONTENTS

LIST OF FIGURES

Figure **Page**

Figure **Page**

Figure **Page**

LIST OF TABLES

Table **Page**

CHAPTER 1

INTRODUCTION

1.1. Introduction and Scope of Study

Piles, known as deep foundations, are generally preferred when the local soil conditions do not have sufficient load-bearing capacity or the loads from the superstructure or design requirements compel a deep foundation application. Depending on the location and purpose of the foundations, they can be made of different types of materials, such as metal, concrete, and timber. Understanding the behavior of piles is crucial as they represent a significant component within the realm of construction.

In general, piles are used in the form of pile groups in which interactions among piles play an essential role in the response of the pile group. Due to such interactions, the load-displacement curve of a pile placed in a pile group will differ from that of a single isolated pile. Such difference does not work in favor of the pile group since the group interaction causes piles to have additional displacement compared to a single isolated pile. Interaction among piles depends on some parameters, such as the pile's location in the group, pile spacing, geometric properties of piles, and material properties of piles and soil in which the pile group is embedded. Therefore, it is crucial to model the response of pile groups accurately and efficiently to account for the effect of the group interactions among piles in a group.

Vallabhan and Mustafa (1996) presented a study about pile-soil interaction for a single isolated pile. Their model was extended by İşbuğa (2023) to consider the interaction between two identical piles, along with the development of an algorithm for the model. The aim of this study is to accurately model pile groups with more than two piles, as well as pile groups featuring both rigid and free head piles while accounting for the interaction among the piles. In this respect, the model proposed by İşbuğa (2023) and the algorithm were further extended to include pile groups.

1.2. Organization of the Thesis

This thesis consists of five chapters. The first section (CHAPTER 1) is an introduction chapter summarizing the thesis studies.

The second section (CHAPTER 2) presents the literature review for pile-soil interaction and pile-soil-pile interaction.

The third section (CHAPTER 3) explains how the pile-soil-pile interaction is applied to pile groups in this study, how the numerical model is created and the working principle of the algorithms using flowchart.

The fourth section (CHAPTER 4) includes the properties of the analyzed pile groups and the comparison of the results with previous studies and finite element method results.

The final part of the thesis (CHAPTER 5) is the conclusion part. This section summarizes all the studies and obtained results.

CHAPTER 2

LITERATURE SURVEY FOR THE SINGLE PILE MODELS AND PILE GROUP MODELS

2.1. Introduction

Modeling the response of piles under various loading conditions is already a challenging task, and there have been studies focusing on pile-soil interaction models in the literature. Winkler (1867), which models the soil layers as discrete springs, is one of the most used among the pile models. In their work, Reese and Seed (1957) assumed that both the pile and the soil possess compressible properties. They proposed that the load is transmitted into the surrounding soil influenced by the relative movement of the pile. Randolph and Wroth (1979) assumed that soil deformation could be described by a logarithmic function which depends on the radial distance *r* from the pile's center. Poulos and Davis (1980) proposed a new approach to the pile-soil interaction assuming that there is no residual stress on the pile and soil due to the installation of the pile. Vallabhan and Mustafa (1996) studied a new model for pile-soil interaction which includes the continuum behavior of soil around the pile. Some models were also extended to model interaction among the piles in the pile groups Mylonakis and Gazetas (1998) extended the Randolph and Wroth (1978) model for grouped piles in layered soil, Cao and Chen (2008) extended the Muki and Sternberg's (1970) model for two pile interaction, also İşbuğa (2023) extended the Vallabhan and Mustafa (1996) single pile model for the two-pile interaction. There are various numerical approaches to model the interaction among the piles, including the boundary element method and the finite element method, which also provides the opportunity to employ the conventional soil plasticity models. However, such numerical tools require expertise in using software to create models and also demand extensive time to create geometry and models for analyses. This time demand increases if multiple try-and-error attempts are involved to derive an optimum pile group design.

One of the earliest works in the field belongs to Poulos (1968). Poulos (1968) defined the interaction factor by dividing the extra settlement due to the neighboring pile by the settlement due to the load carried by the pile. Poulos (1968) developed a model for

analyzing pile groups by superposition approach to obtain the interaction factor. Butterfield and Banerjee (1971) presented a rigorous model for compressible and rigid pile groups with floating pile caps. Randolph and Wroth (1979) introduced an approximate analytical solution that relies on the superposition of single pile displacements. Mylonakis and Gazetas (1998), presented a solution by employing the Winkler (1867) model of soil response. Chen et al. (2011) extended the Muki and Sternberg (1970) model by employing a Fredholm integral equation to investigate the interaction between two vertically loaded piles.

Vallabhan and Mustafa (1996) introduced an approach that facilitates a comprehensive analysis of the interaction between piles and the surrounding soil. This approach considers the deformation characteristics and stresses across the entire soil medium.

Isbuga (2023) presented a model that considers the pile-soil-pile interaction by extending the method proposed by Vallabhan and Mustafa (1996). This study further presents a new algorithm to model axially loaded pile groups by extending the interaction model proposed by Isbuga (2023) for pile groups with different numbers of piles. This study compares the results of the present model with the finite element method and those of previous models existing for various cases in the literature.

2.2. Pile-Soil Interaction

2.2.1. Winkler Model (1867)

The Winkler (1867) model is an idealization that considers the soil as a system of springs, which undergo displacement in response to the applied load. Soil can have linear or nonlinear stress-strain behavior in the model. In the Winkler (1867) model, the springs are limited to vertical displacement and are attached to two nodes, with the lower nodes being fixed in place. The main limitation of the Winkler (1867) model is that it neglects the soil's shear capacity. By disregarding shear stresses, the model does not account for the lateral spreading of displacement in the transverse direction. Due to the neglected shear capacity of soils, the Winkler (1867) model assumes displacement discontinuity between loaded and unloaded surfaces (Teodoru and Bogdan, 2009). However, in reality, soil has shear capacity, and as a result, no displacement discontinuity occurs in practice

(Aron and Jonas, 2012). The discontinuity in the mentioned displacements is shown in Figure 2.2, the difference between the Winkler model and the soil behavior in practice can be seen.

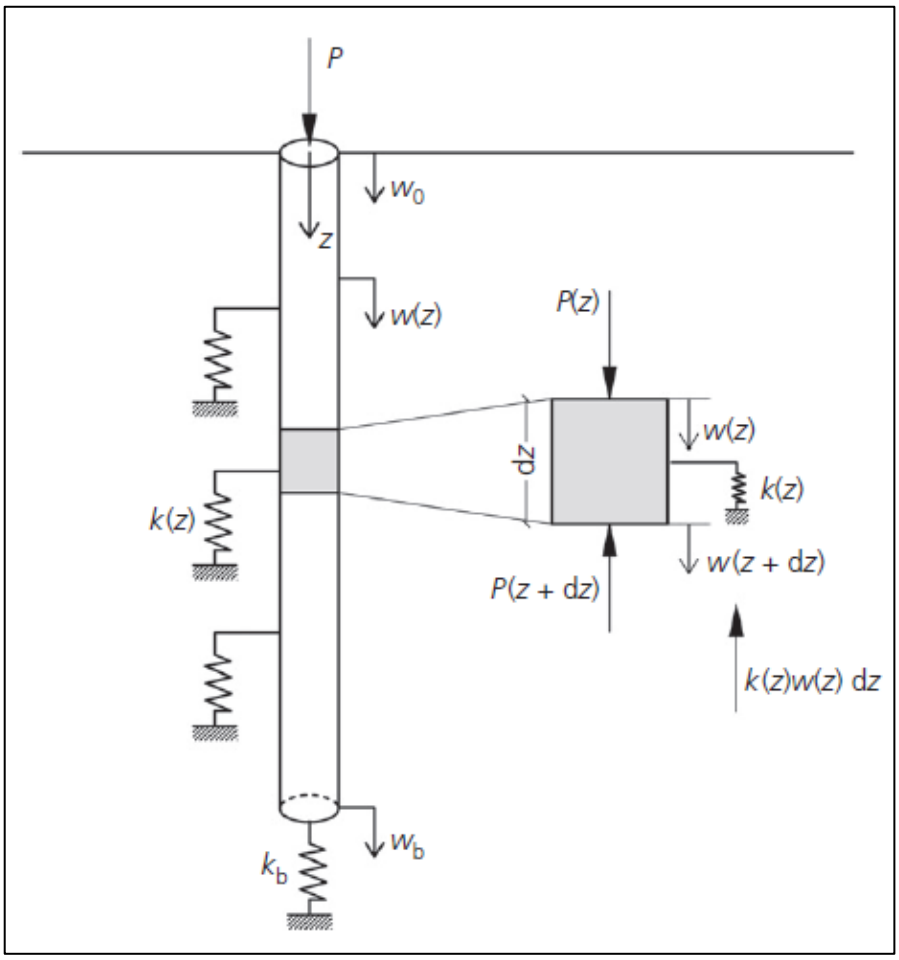

Figure 2.1 The Winkler model for a pile under axial loading

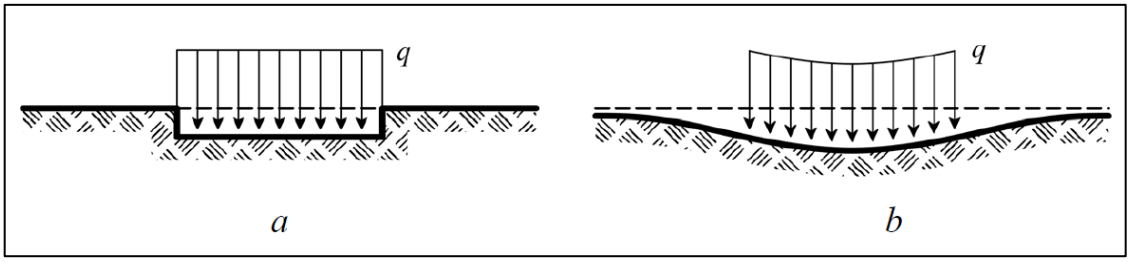

Figure 2.2 Behaviour of elastic foundations under uniform load: a – Winkler model, b – deflection of soil foundation (Teodoru and Bogdan, 2009)

2.2.2. Reese Model (1964)

Seed and Reese (1957) investigated the behavior of the axially loaded pile and the surrounding soft clay. Seed and Reese (1957) assume that the pile is compressible, and the amount of load that is transferred into the soil surrounding the pile is influenced by the pile's movement relative to the surrounding soil. Reese (1964) uses *t-z* curves. The behavior of the soil-pile interface is described in terms of displacement and shear stress by *t-z* curves. In Figure 2.3, the illustration represents the pile as a deformable body, with the soil replaced by mechanisms demonstrating the nonlinearity of unit load transfer in skin friction concerning the pile's movement. The unit load transfer is described by a set of *t-z* curves where t denotes the load transfer inside resistance at a specific point along the pile, and *z* represents the displacement of that point relative to its initial position before loading.

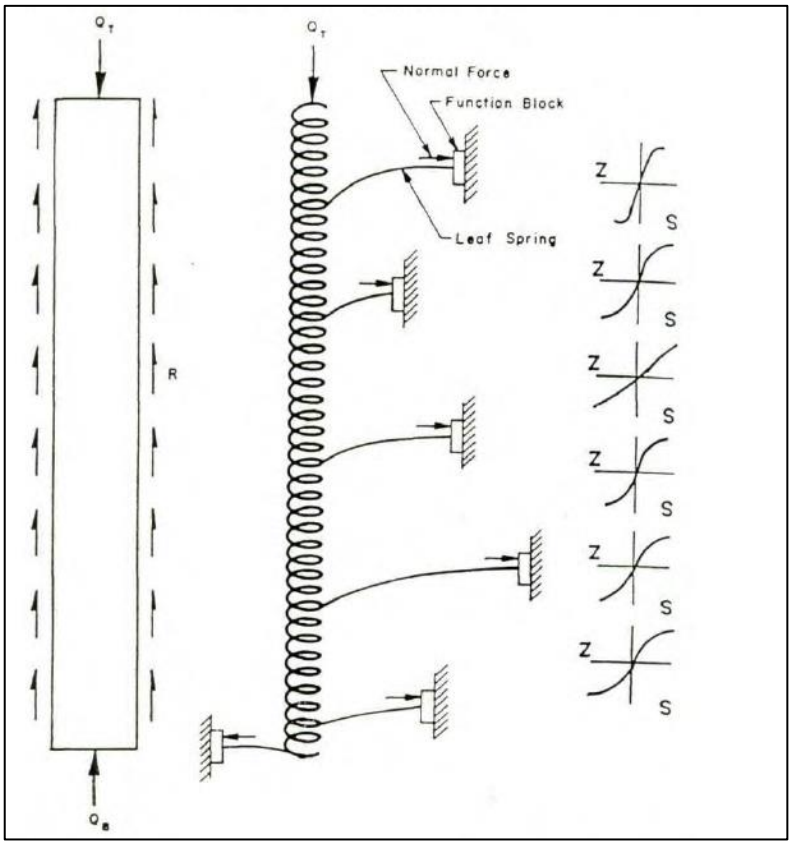

Figure 2.3 Model of axially loaded pile (Reese, 1964)

In Figure 2.4, the dashed line represents the applied stress, which diminishes as the distance from the pile wall increases. At a certain distance away from the pile, the

applied stress matches the shearing resistance of the clay, and when the pile is under full load, there is a likelihood of sliding to occur.

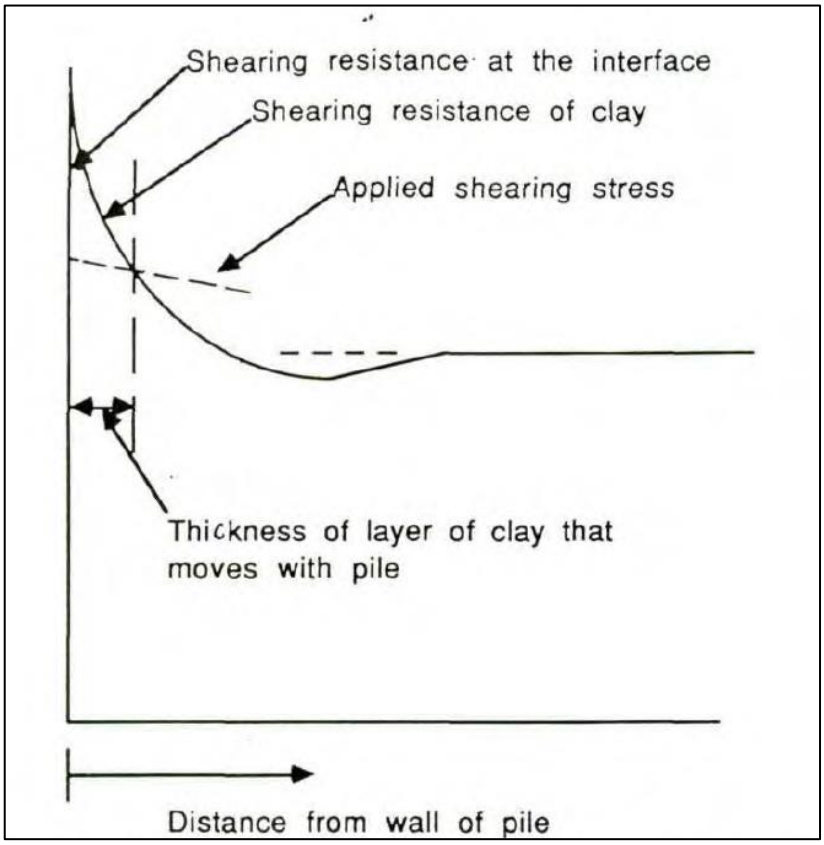

Figure 2.4 Conceptual curves for locating the position of failure (Seed and Reese,1957)

2.2.3. Vallabhan and Mustafa (1996)

Vallabhan and Mustafa (1996) are a valuable addition to the widely recognized Reese(1964) model, which utilizes *t-z* curves to study the settlement of axially loaded piles. Unlike the Reese (1964) model, Vallabhan and Mustafa (1996) incorporate the continuum behavior of the soil, treating it as a continuous medium with linear elastic properties. This approach enables a comprehensive analysis of the interaction between the pile and the surrounding soil, taking into account the deformation characteristics and stresses in the entire soil medium.

The model by Vallabhan and Mustafa (1996) offers a comprehensive understanding of the settlement behavior of axially loaded piles in soft clay. The model introduces a method to calculate the axial settlement of piles by employing a variational approach and minimizing a potential energy functional. In this model, it is assumed that

there is perfect compatibility of displacements between the pile and the surrounding soil at the interface between them, also both pile and soil behave linearly. The derived equations in Vallabhan and Mustafa (1996) corroborate the initial empirical assumptions that were made by Reese (1964). In contrast to the Reese (1964) model, the model proposed by Vallabhan and Mustafa (1996) takes into account not only the shear stresses in the surrounding soil but also regards the presence of a compressive strain in the soil, which was previously disregarded.

This model ignores the radial displacement of the soil because it is negligible compared to vertical displacement. The assumption is made that the vertical displacement of the soil at any point surrounding the pile could be obtained. This feature of the model made it possible to employ this approach to model interaction between two piles and, in turn, interaction among all the piles in the pile groups. Isbuga (2023) proposed using Vallabhan and Mustafa (1996) model to model the interaction between two piles and proposed the formulation, and also developed an algorithm to employ the model in a Python computer code. The details of Vallabhan and Mustafa (1996) and Isbuga (2023) are presented in the following chapters.

2.2.4. Randolph and Wroth (1978)

In previous research on the soil-pile interface, shear strains around the pile were assumed to be confined within a limited softened zone. Randolph and Wroth (1978) proposed a sufficient semi-analytical model, which assumes that the soil deformation can be described using a logarithmic function that depends on the radial distance r from the center of the pile (Vallabhan and Mustafa, 1996). In this model, the behavior of the soil around the pile and below the pile base is treated differently. This approach is shown in Figure 2.5.

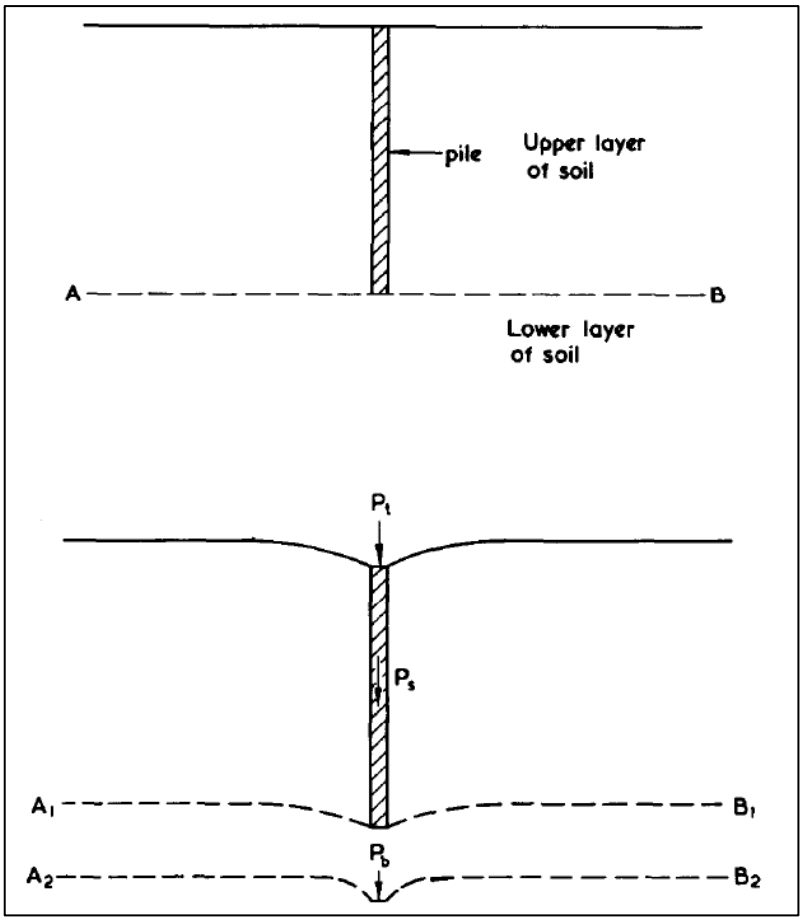

Figure 2.5 Top and bottom soil layers behaviour (Randolph and Wroth, 1979)

AB line divide soil layers into two, one is surrounding the pile and the other is below the pile base, as shown in Figure 2.5. The model assumes that the soil above point AB will undergo deformation solely due to the stresses transferred from the pile shaft, while the soil below point AB will deform solely because of the stresses at the pile base (Randolph and Wroth, 1978).

2.2.5. Poulos and Davis (1980)

Poulos and Davis (1980) conducted a review of work completed until 1980. In their work, they considered a cylindrical pile loaded with an axial load *P* at the ground surface. For the analysis, the pile is subjected to a system of uniform shear stresses around its periphery, while the base experiences uniform vertical stress (Poulos and Davis, 1980). In this analysis, it is assumed that both the pile and the soil are initially stress-free and that there are no residual stresses due to the pile installation. Both the soil and the pile are considered to behave linearly elastic. The pile's sides' roughness ensures deformation

compatibility between the pile shaft and the surrounding soil. At the pile-soil interface, no slip occurs, and it remains elastic. Thus, the displacements of the pile and the neighbouring soil must be same to maintain compatibility between them.

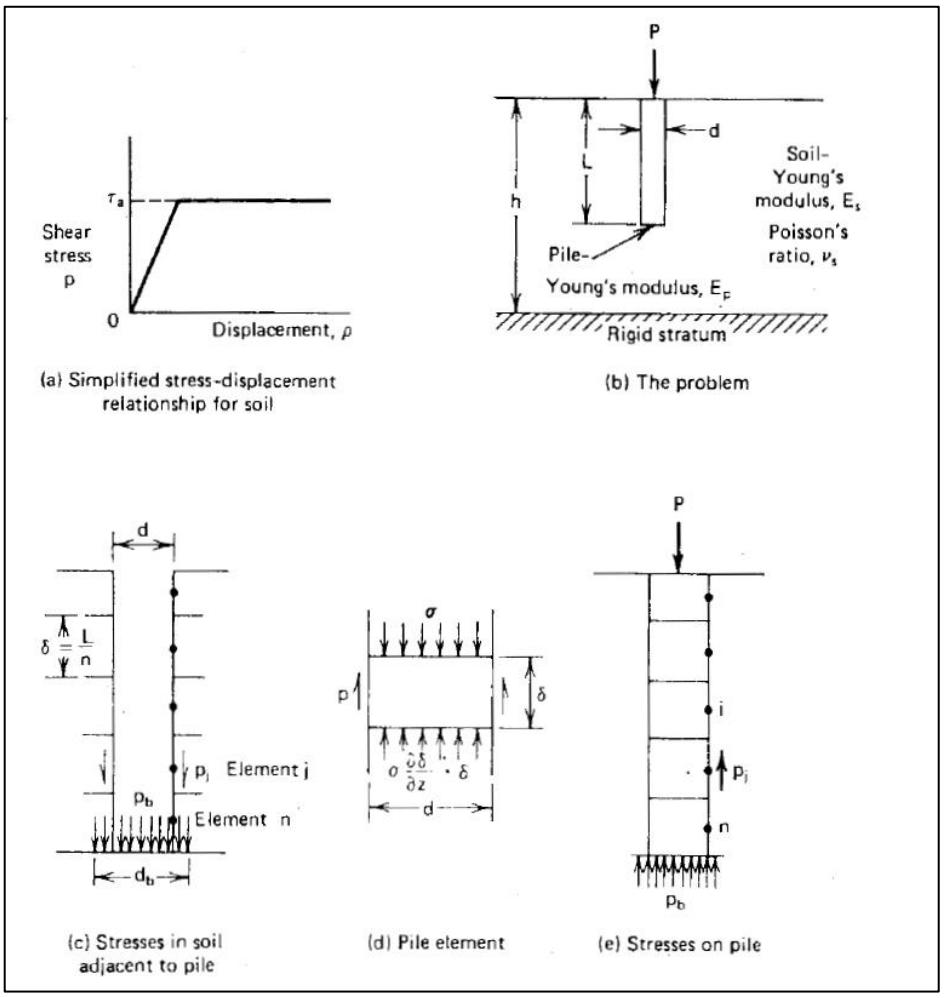

Figure 2.6 Analysis of floating pile (Poulos and Davis, 1980)

In the model, the soil is assumed to possess linear elastic properties, homogeneity, and isotropy. The soil is considered semi-infinite, extending infinitely in all directions. Furthermore, the displacements at the pile-soil interface are assumed to be adaptable, ensuring that there are no discontinuities or slips between the pile and the surrounding soil.

2.3. Pile-Soil-Pile Interaction

Piles are generally used in the form of groups to transfer the load from structure to soil. The behavior of piles in groups is different from that of single piles, depending on the pile spacing. When a pile is loaded, it disturbs the soil around the pile and creates a displacement field in the soil surrounding the pile. These fields can overlap depending on the spacing of the piles as seen in Figure 2.7 and this situation increases the settlement of piles. This interaction mechanism has attracted the attention of researchers, and various studies have been conducted on the subject. The interaction behavior was described using the interaction factor, which has been widely adopted by researchers. The one initially proposed by Poulos (1968) is the most prevalent among various interaction factors. Poulos (1968) defines the interaction factor by dividing the extra settlement because of the neighboring pile to settlement due to the load carried by the pile itself. Some of the pioneering and recent works in the field include Poulos (1968), Butterfield and Banerjee (1971), Randolph and Wroth (1979), Chow (1986), Mylonakis and Gazetas (1998), and Chen et al. (2011) presented research on pile-soil–pile interaction. The following sections will discuss these models.

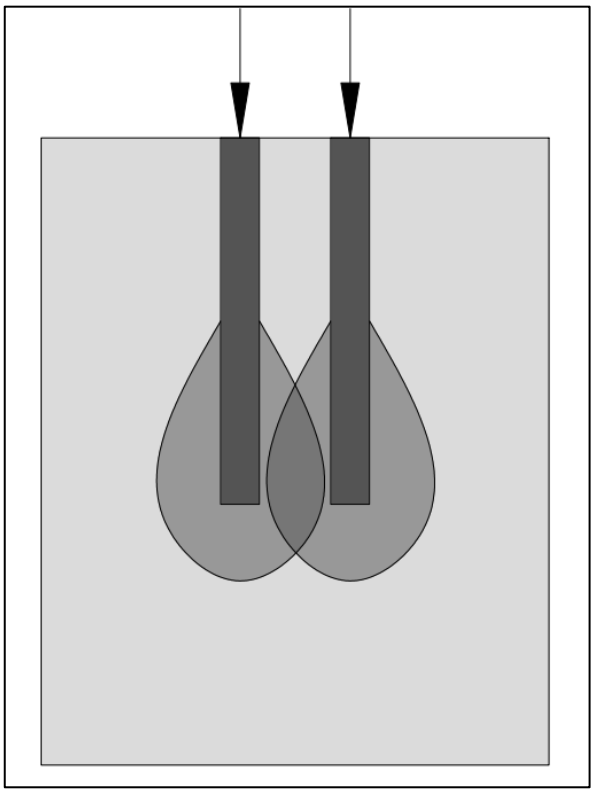

Figure 2.7 Overlapping zone in two piles (Das B. M., 2016)

2.3.1. Poulos (1968)

Poulos (1968) conducted a settlement analysis to characterize the interaction between two piles in an elastic soil. He quantified the additional settlement experienced by each pile due to the interaction effect, expressing it in terms of an interaction factor. Additionally, Poulos (1968) demonstrated that for pile groups showing symmetrical behaviour (all piles settle and load equally), the change in settlement caused by the interaction can be determined by simply superposing the values of the interaction factors for each pile within the group. This simplification allows for an efficient analysis of settlement behavior in such pile configurations (Poulos and Davis, 1980). During his study, Poulos (1968) investigated two distinct scenarios: one with piles having a rigid pile cap, and the other with piles having a flexible pile cap. In the flexible pile cap case, each pile in the group has an equal load, and the interaction factor can be utilized to account for the interaction effects among the piles. However, in the case of a rigid pile cap, where all the piles in the group experience the same settlement, the interaction factor cannot be directly applied. Instead, a group reduction factor (R_g) is used to consider the group effect on settlement behavior. To model the pile shaft load, Poulos (1968) employed a method where he replaced it with uniform vertical shear stress applied on each pile elements' surface. The discontinuity of the model results from the existence of the piles in soil was neglected. In his study, Poulos (1968) employed two different values for Poisson's ratio to investigate the effects of soil stiffness on pile group behavior. By using these different values, the researcher ought to understand how the variation in Poisson's ratio influences the settlement and interaction effects within the pile group. Furthermore, to validate the accuracy and reliability of his analytical findings, Poulos compared his research results with field data. Indeed, Poulos (1968) not only captured the correct trends in pile group behavior but also yielded quantitative values that showed reasonably close agreement with the observed values from field data.

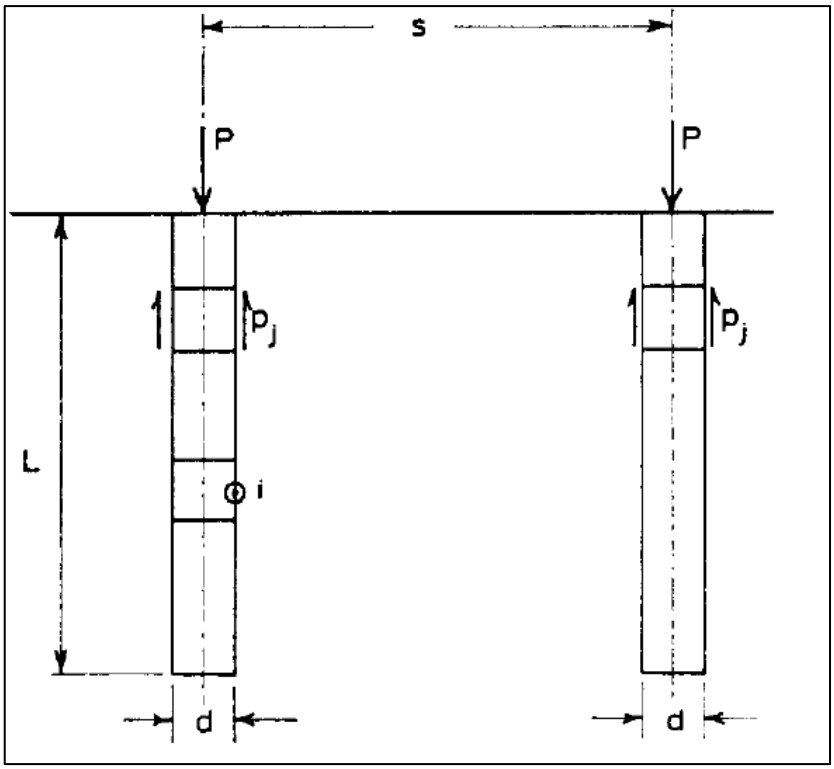

Figure 2.8 Group of two piles (Poulos, 1968)

2.3.2. Butterfield and Banerjee (1971)

Butterfield and Banerjee (1971) presented an analytical approach that is elaborated upon and extended to examine the behavior of axially loaded rigid and compressible pile groups that have floating caps positioned in an arbitrary manner. Butterfield and Banerjee (1971) demonstrated that significant errors occur in the computed values of radial stress components near a loaded pile when assuming that the disruption caused by the presence of the piles in the elastic half-space is neglected. They presented the results of their research through a set of graphs illustrating the impact of varying pile properties and soil properties, and the relationship of the load-displacement and base enlargement behavior of single axially loaded piles (Butterfield and Banerjee, 1971). Butterfield and Banerjee (1971) obtained similar results for the group reduction factor as those presented in Poulos (1968).

2.3.3. Randolph and Wroth (1979)

Randolph and Wroth (1979) presented an approximate analytical approach for calculating the vertical deformation of a group of piles. This method relies on superimposing the displacement patterns of single piles within the group (Chen et al, 2011). The technique relies on combining the displacement patterns of single piles through superposition. Their work involves treating the average behavior along the pile shafts independently from the behavior beneath the pile base. The soil was represented as an elastic material defined by a shear modulus, presumed to change linearly with depth, along with a constant Poisson's ratio (Randolph and Wroth, 1979). There is a displacement field around each single pile, and if the displacement field of a pile crosses another pile's displacement field like in Figure 2.7, the displacement of piles will increase. They propose that the interaction factors between two piles at a specific pile spacing could be determined through integral equation analysis, assuming all of the piles in the group should be the same length. Consequently, a pile group could be analyzed by constructing a matrix of interaction factors for each pair of piles within the group.

2.3.4. Mylonakis and Gazetas (1998)

Mylonakis and Gazetas (1998) studied pile–soil–pile interaction in layered elastic soil. They devised an analytical method by employing the Winkler model of soil response to compute the vertical interaction factors between two piles positioned within a soil composed of multiple layers. Mylonakis and Gazetas (1998) demonstrate that these interaction factors are influenced by not just the displacement pattern resulting from the subsidence of a loaded ('source') pile, but also by the relationship between the neighboring ('receiver') pile and the soil affected.

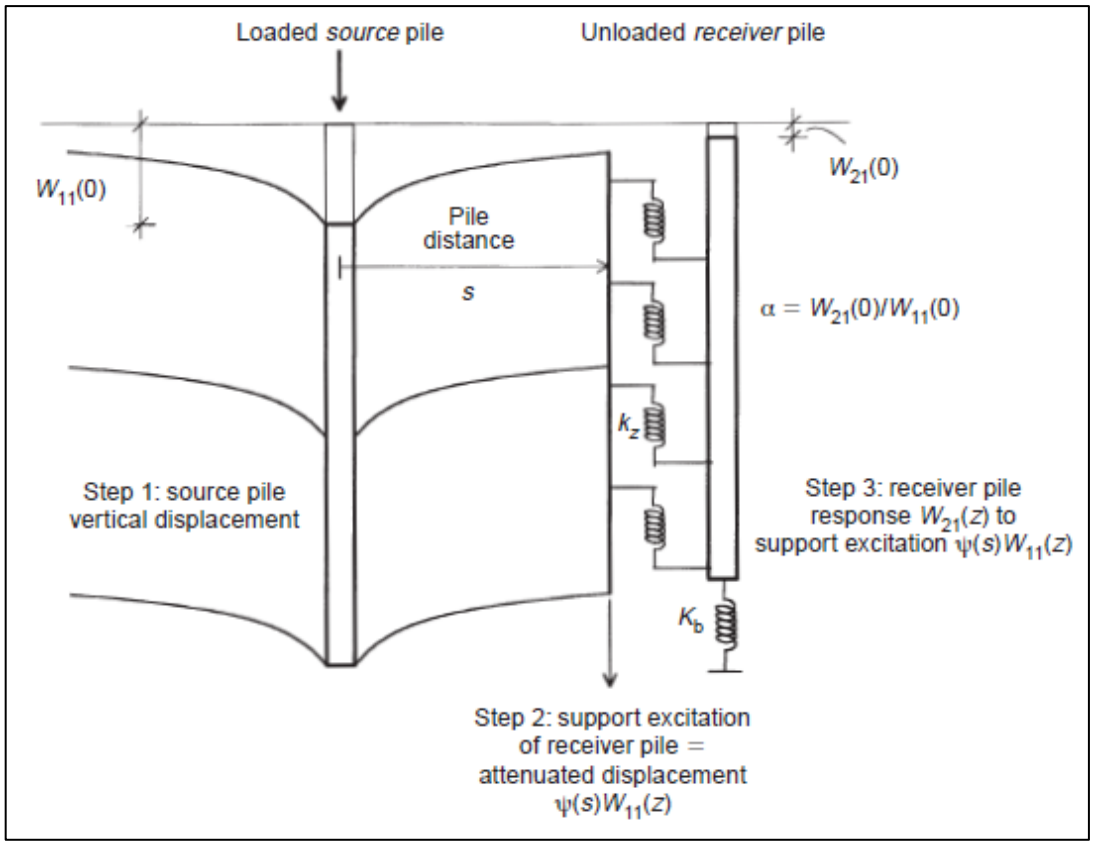

Figure 2.9 Influence of source pile (loaded) on the receiver pile (unloaded pile). (Mylonakis and Gazetas, 1998)

In order to simulate the interaction between the receiver pile and the soil, the receiver pile is represented as a beam that is supported with Winkler springs as seen in Figure 2.9. The loading of these springs originates from the attenuated soil displacement.

2.3.5. Chen, Song, and Chen (2011)

Muki and Sternberg (1970) introduced a method to examine the interaction between soil and piles, utilizing the concept of a fictitious pile-extended half-space model. Chen and Cao (2008) expanded upon the model proposed by Muki and Sternberg (1970) to address the case of two vertically loaded piles that are embedded within a soil half-space as seen in Figure 2.10. Their assumption was that the axial strains present in the fictitious piles match those occurring at the center points within the corresponding extended soil (Cao and Chen, 2008). Their model was limited to situations involving semi-infinite soil and thus lacked direct applicability when considering piles embedded within a finite soil layer. The approach proposed by Chen et al. (2011) represents a further

development of the model introduced by Cao and Chen (2008). They employed the Fredholm integral equation of the second kind to describe the unknown axial forces along the hypothetical piles and subsequently resolved this equation through numerical techniques. They conducted a comparison between their results and those presented by Poulos and Davis (1980), along with those from Mylonakis and Gazetas (1998).

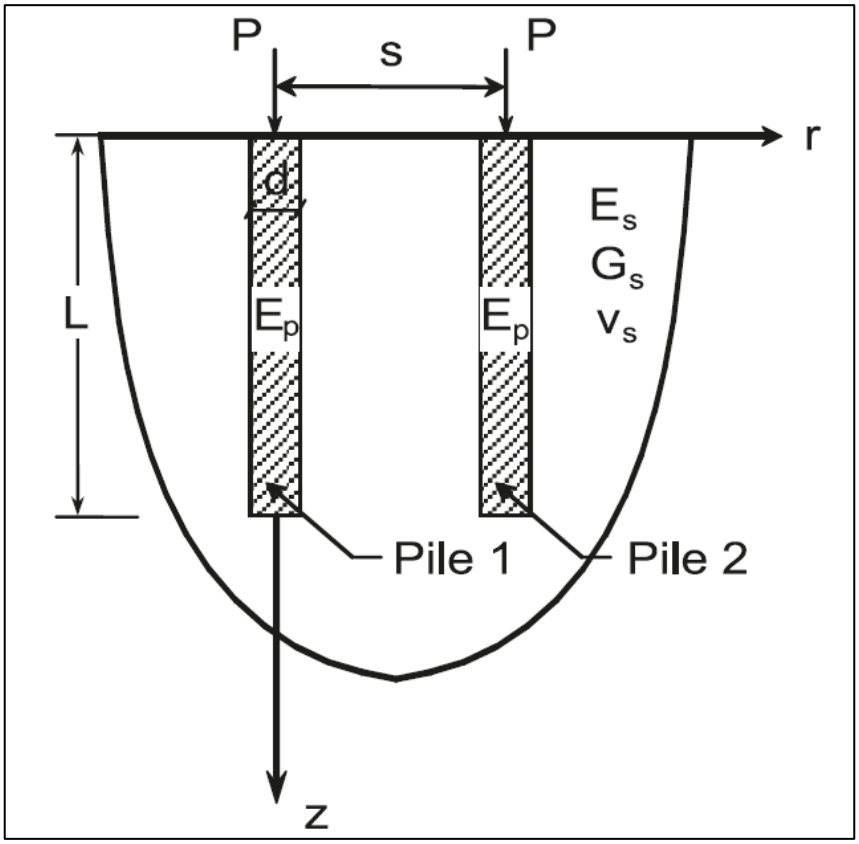

Figure 2.10 Geometry of piles and embedding soil medium (Chen et al., 2011)

CHAPTER 3

THE NUMERICAL APPROACH USED TO MODEL PILE GROUPS AND THE ALGORITHMS

3.1. Introduction

A numerical model comprises a multitude of mathematical equations that rely on computer-based calculations to approximate solutions for the underlying physical problem (Zafarparandeh and Lazoglu, 2012). The general classification of numerical methods is shown in Figure 3.1.

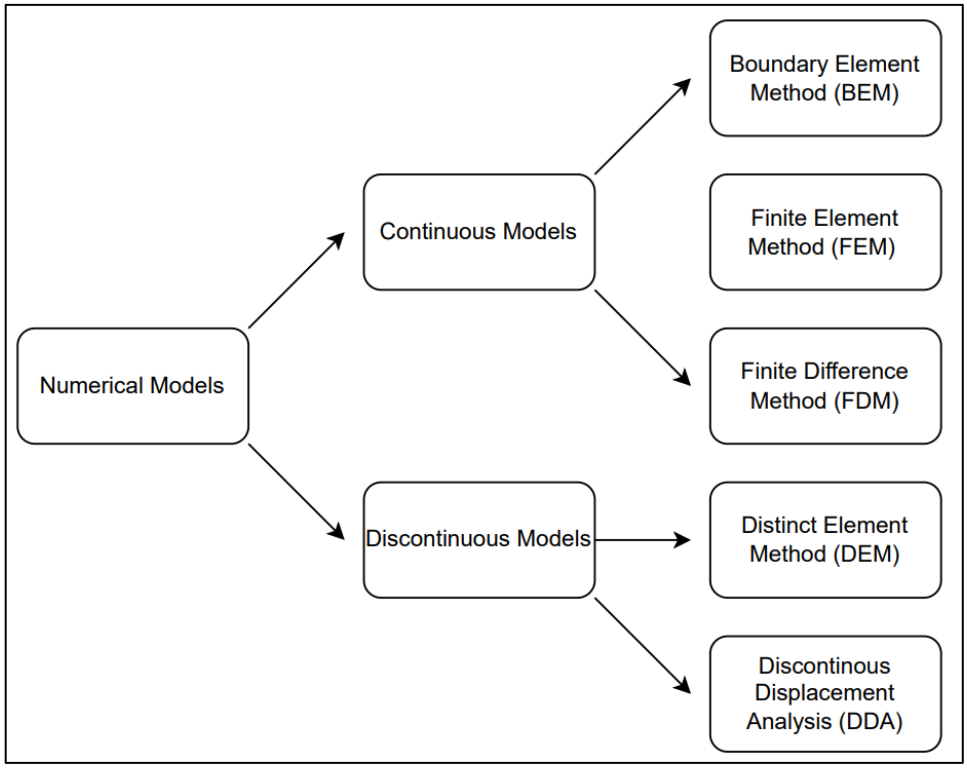

Figure 3.1 General classification of numerical methods (Thote et al., 2016)

A continuous model is a mathematical representation of the problem or system that has continuous variables and generally, it is useful for such systems where changes in variables are smooth. This contrasts with discrete variables, which can only take on distinct, separate values. The Finite Element Method (FEM) is a numerical technique used

to solve engineering and mathematical problems. The FEM divides a complex problem into simpler, smaller elements (thus the name finite elements) that are easier to analyze (Chapra and Canale, 2010). The boundary element method (BEM) is a numerical technique where the boundary surrounding a region is divided into elements, as opposed to the finite element method, which divides the region itself into elements (Pincus, 2003). The finite difference method (FDM) is an approximate method for solving differential equations by discretizing the domain into a grid of points the finite difference method has found application in solving a broad spectrum of problems (Zhou, 1993). In this thesis, the finite difference method is used as a numerical modeling method.

3.2. Finite Difference Method

In the finite difference method, the derivatives present in the differential equation are estimated using finite difference formulas. The interval [a, b] can be partitioned into *n* equal subintervals of length *h*, as illustrated in Figure 3.2.

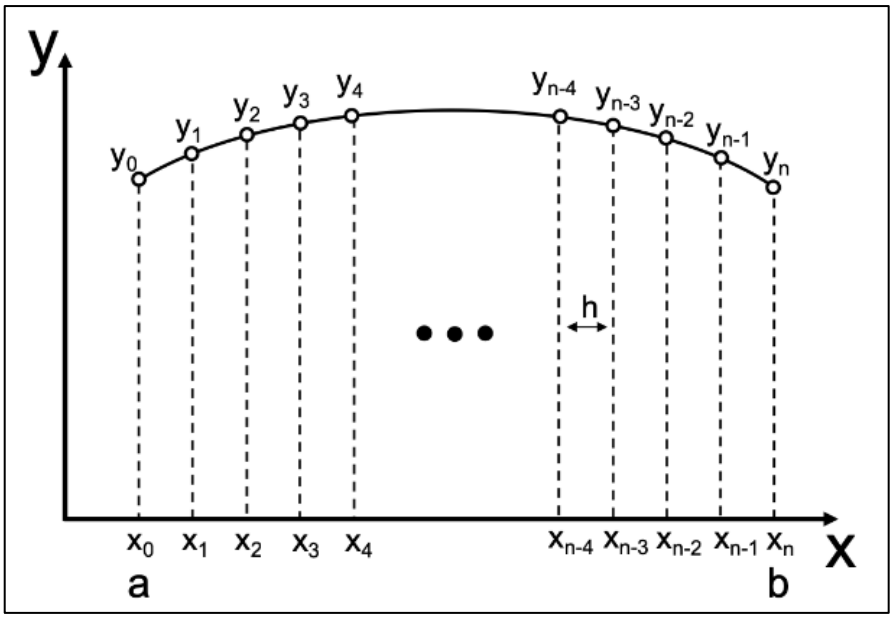

Figure 3.2 Finite difference method example on the curve (Kong et al., 2020)

Derivatives of differential equations are approximated by using finite differences. Backward difference, forward difference, and central difference methods can be used. Generally, the accuracy of the central difference method is higher than that of the

backward and forward difference methods (Zhou, 1993). In this study, the central difference method was used.

The central difference formula in the finite difference method is given by:

$$\frac{dy}{dx} = \frac{y_{i+1} - y_{i-1}}{2\mathrm{h}} \tag{3.1}$$

$$\frac{d^2y}{dx^2} = \frac{y_{i+1} - 2y_i + y_{i-1}}{\mathrm{h}^2} \tag{3.2}$$

3.3. Finite Element Method

Finite Element Method (FEM) is a powerful numerical technique employed to solve diverse engineering and physical problems, particularly those that can be described by partial differential equations. FEM is widely used across various fields, including structural analysis, fluid dynamics, heat transfer, and more, as it provides a versatile and efficient means to approximate and analyze complex real-world phenomena. This method subdivides a problem's domain into smaller, discrete elements, allowing for the accurate approximation of solutions to partial differential equations (Reddy, 2005). Within each element, the field variable (e.g., displacement or temperature) is approximated using interpolation functions. These functions typically take the known values of the field variable at the element's nodes and create a continuous approximation within the element (Logan, 1986). The governing partial differential equation is converted into a weak form or variational formulation. This typically involves multiplying the partial differential equation by a weight function and integrating it over the domain. The aim is to find a solution that minimizes the error. Individual contributions from all the elements are integrated to create a comprehensive system of algebraic equations. This process entails the assembly of the element equations into a single global stiffness matrix (Ern and Guermond, 2004). The resulting system of equations is solved using numerical techniques.

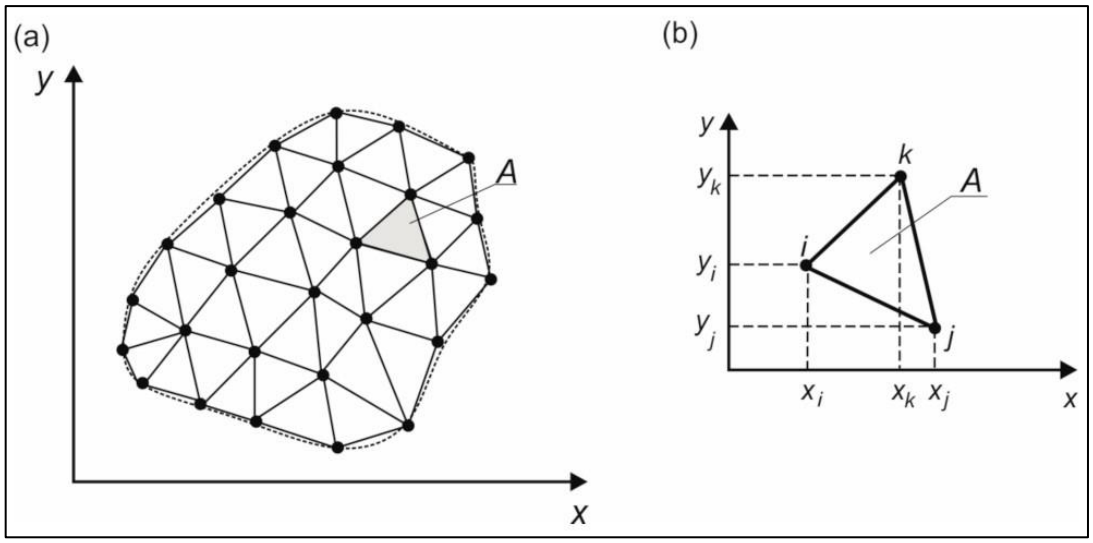

Figure 3.3 Finite element method discretization, (a) discretized domain, (b) discrete element of domain (Gąsiorowski, 2022)

Discretization of the domain by triangular mesh and triangular element is shown in Figure 3.3.

3.4. Mathematical Formulation of the Single Pile Model

This section provides a detailed explanation of the mathematical formulation of the model introduced by Vallabhan and Mustafa (1996), this model is used to analyze isolated single piles. The theory presented here was initially devised by Vallabhan (1994), with the objective of investigating the linear elastic load-settlement behavior of piles. The formulation shows similarity to the approach employed for analyzing slabs and beams on elastic foundations, as introduced by Vallabhan et al. (1991). Utilizing the boundary conditions and field equations, Vallabhan and Mustafa (1996) introduced a solution in closed form. This closed-form solution facilitates the identification of the key non-dimensional parameters which control the behavior of all system.

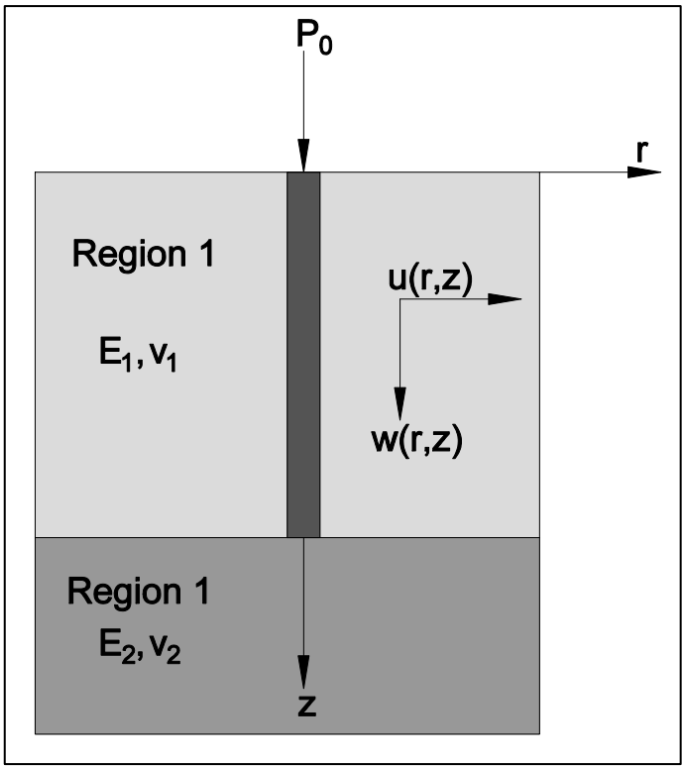

Figure 3.4 Pile and the soil medium (Vallabhan and Mustafa, 1996)

The system is shown in Figure 3.4, there is an isolated single pile embedded in layered soils. The first layer extends through the pile shaft and surrounds the pile; the second layer is underneath the pile shoe and provides bearing resistance. Young's modulus and Poisson's ratio of soils can be different, as indicated in Figure 3.4. The cross-sectional area, radius, length, and Young's modulus of the pile are *Ap*, *R*, *l*, and *Ep*, respectively. The model is axisymmetric and as stated in the literature, Vallabhan and Mustafa (1996) assumed radial displacement (u(r,z)) is negligible compared to the vertical displacement (w(r,z)) in the soil. Moreover, the assumption is made that the vertical displacement at any given point within the soil encompassing the pile can be represented as follows:

$$w(r,z) = w(z)\emptyset(r) \tag{3.3}$$

The total potential energy of the system in this model given as:

$$\varphi = U_{pile} + U_{soil} - Pw(0) \tag{3.4}$$

$$= \frac{1}{2}\int_0^l E_p A_p \varepsilon_z^2 dz + \frac{1}{2}\int_{soil}\iint \sigma_{ij}\varepsilon_{ij} dvol - Pw(0) \quad (3.5)$$

Taking variations of w and ∅ using variational calculus after substituting for the stresses and strains, the following equation was obtained by Vallabhan and Mustafa (1996):

$$-\left(E_p A_p + 2t_1\right)\frac{d^2 w}{dz^2} + k_1 w = 0, for\ 0 < z < l \quad (3.6)$$

Boundary conditions:

$$at\ z = 0,\ -\left(E_p A_p + 2t_1\right)\frac{dw}{dz} = P_0 \quad (3.7)$$

$$at\ z = l,\ -\left(E_p A_p + 2t_1\right)\frac{dw}{dz} = Kw_1 \quad (3.8)$$

$$where\ K = \sqrt{[k_2(E_2\pi R^2 + 2t_2)]} \quad (3.9)$$

In the above equations:

$$k_i = 2\pi G_i \int_R^\infty r\left(\frac{d\emptyset}{dr}\right)^2 dr \quad (3.10)$$

$$t_i = 2\pi E_i \int_R^\infty r\emptyset^2 dr \quad (3.11)$$

Two regions of the soil are shown by subscripts i=1,2. The field equation for the soil domain is:

$$r\frac{d}{dr}\left(r\frac{d\emptyset}{dr}\right) - \frac{n}{m}r^2\emptyset = 0,\ \ for\ R < r < \infty \quad (3.12)$$

with boundary conditions:

$$at\ r = R,\ \emptyset = 1 \quad (3.13)$$

$$at\ r = \infty,\ \frac{\mathrm{d}\emptyset}{dr} = 0 \quad (3.14)$$

the functions *m* and *n* are:

$$m = 2\pi G_1 \int_0^l w^2 dz + \pi G_2 \frac{w_l^2}{\alpha} \quad (3.15)$$

$$n = 2\pi E_1 \int_0^l \left(\frac{dw}{dz}\right)^2 dz + \pi E_2 \alpha w_l^2 \quad (3.16)$$

where

$$\alpha = \sqrt{\left[\frac{k_2}{(E_2 \pi R^2 + 2t_2)}\right]} \tag{3.17}$$

The equations in this model were developed by Vallabhan and Mustafa (1996) through the application of energy principles, taking into account the assumptions made for the displacements.

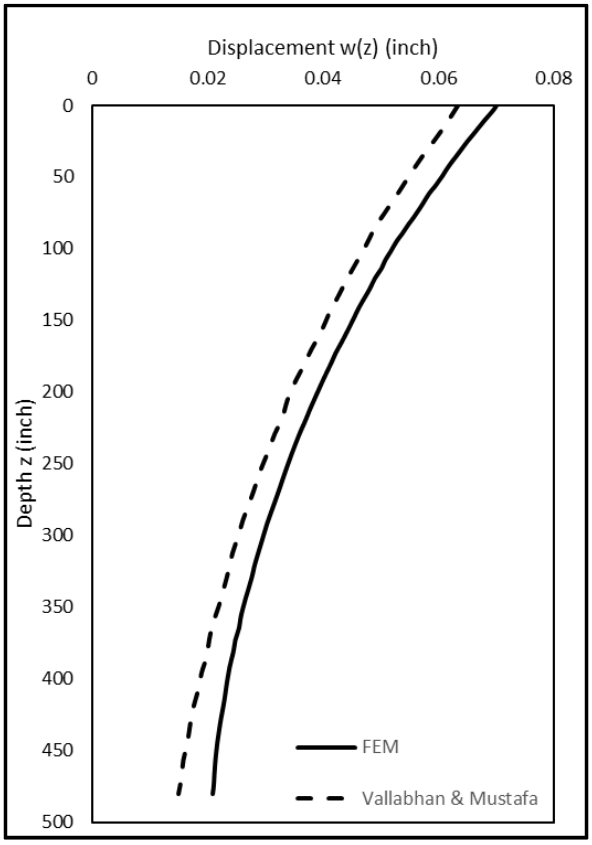

Figure 3.5 Axial displacement vs depth (Vallabhan and Mustafa, 1996)

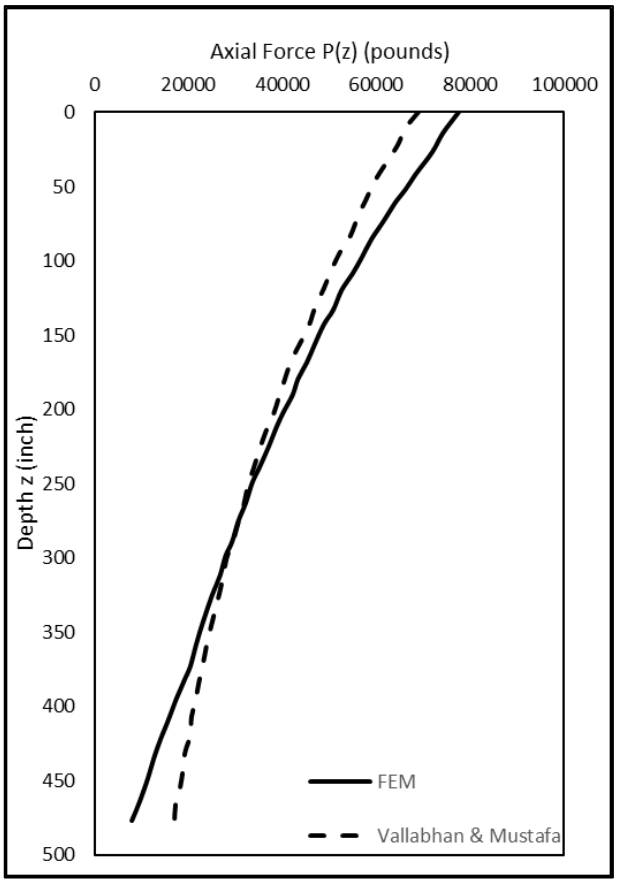

Figure 3.6 Axial force vs depth (Vallabhan and Mustafa, 1996)

It's evident that the outcomes of this model (Figure 3.5 and Figure 3.6) demonstrate a reasonable level of agreement with those produced by a more sophisticated finite element model.

3.5. Mathematical Formulation of the Two-Pile Interaction Model

İşbuğa (2023) proposed that Vallabhan and Mustafa (1996), which accounts for both pile and soil displacement around the pile, can be effectively utilized for modeling the interaction between two identical piles embedded in the same soil. Figure 3.7 depicts the novel interaction model between the two piles examined by İşbuğa (2023). In Figure 3.7, S represents the center-to-center radial distance (pile spacing) between the piles, and w_s symbolizes the soil displacement at the location of the receiver pile.

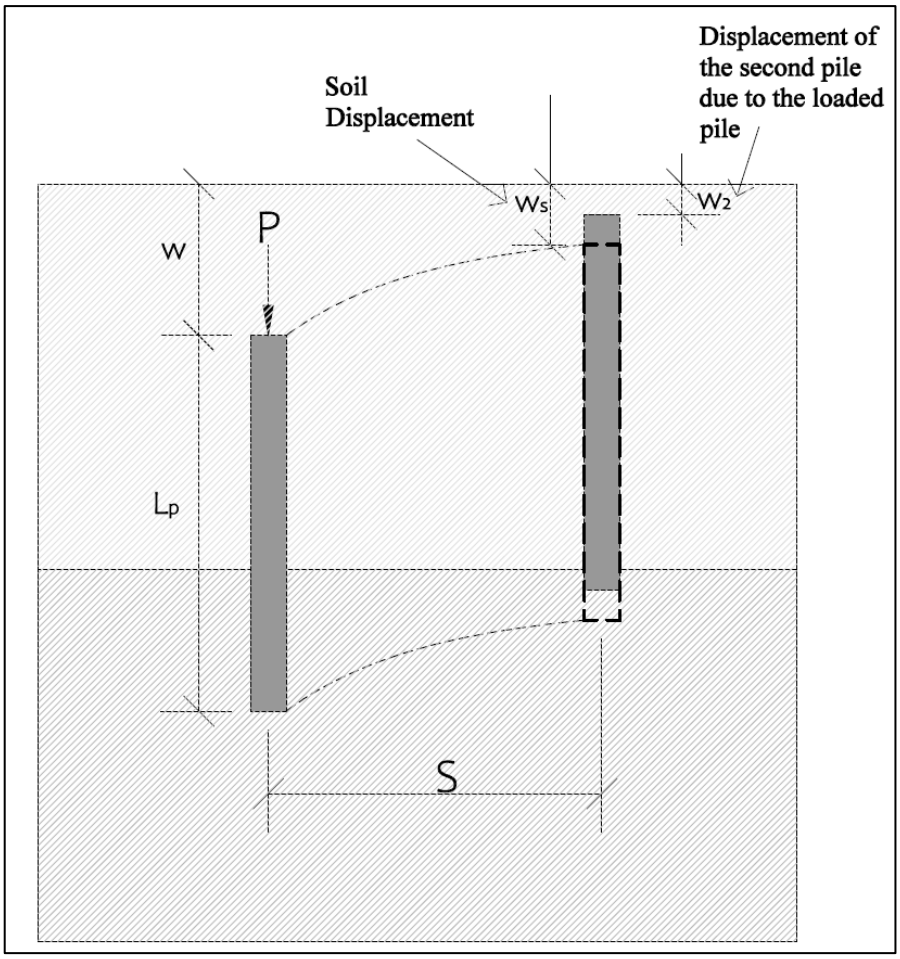

Figure 3.7 Pile-soil-pile interaction between two piles (İşbuğa,2023)

According to İşbuğa (2023) by assuming that both piles share the same material and geometric properties, the governing differential equation provided for a single pile in Equation 3.6 can be adapted to incorporate this interaction as follows:

$$-E_p A_p \frac{d^2 w_2}{dz^2} - 2t_1^{(2)} \frac{d^2(w_2 - w_s)}{dz^2} + k_1^{(2)}(w_2 - w_s) = 0 \tag{3.18}$$

In Equation 3.18, w_2 represents the displacement of the receiver pile, which arises as a result of the loading imposed by the source pile. In this model, he takes into account that the soil reaction varies with respect to relative displacement, so boundary conditions are modified as mentioned:

$$at\ z = 0,\ -E_p A_p \frac{dw_2}{dz} - 2t_1^{(2)} \frac{d(w_2 - w_s)}{dz} = 0 \tag{3.19}$$

$$at\ z = L, -E_p A_p \frac{dw_2}{dz} - 2t_1^{(2)} \frac{d(w_2 - w_s)}{dz} = K^{(2)}(w_2 - w_s)_{L_p} \tag{3.20}$$

Where $2t_1^{(2)}$ and $k_1^{(2)}$ are the soil parameters for the second pile and $K^{(2)}$ is defined as the same as given in Equation 3.6 but using the soil parameters $2t_1^{(2)}$ and $k_1^{(2)}$ for the receiver pile.

3.6. Mathematical Formulation of the Pile Group Model

In this study, İşbuğa (2023) has been further extended to consider the behavior of pile groups that have any number of piles. Two different algorithms were developed for this model, one of them for pile groups with free-head and the other one is pile groups with rigid pile cap.

Equation 3.18 has been revised in this respect since a pile in pile groups will interact with all the other piles around it, so there is more than one pile affecting the pile. Each pile will create a soil displacement field, and to find soil displacement at the location of the receiver pile, soil displacement caused by each pile at the location of the receiver must be summed up. This process should be done for each pile in the group (each pile is also a receiver pile).

$$-E_p A_p \frac{d^2 w_i}{dz^2} - 2t_1^{(2)} \frac{d^2(w_i - \sum w_s)}{dz^2} + k_1^{(2)}(w_i - \sum w_s) = 0 \qquad (3.21)$$

In equation 3.21, the $\sum w_s$ means soil displacement created at the location of the receiver pile by all neighboring piles. For example, consider a pile group consisting of 4 piles. Soil displacement due to the loading of the other three piles in the region of the first pile here is $\sum w_s$. Also, boundary conditions will be modified because in this model pile has more neighboring piles.

$$at\ z = 0,\ -E_p A_p \frac{dw_i}{dz} - 2t_1^{(2)} \frac{d(w_i - \sum w_s)}{dz} = 0 \qquad (3.22)$$

$$at\ z = L, -E_p A_p \frac{dw_i}{dz} - 2t_1^{(2)} \frac{d(w_i - \sum w_s)}{dz} = K^{(2)}(w_i - \sum w_s)_{L_p} \qquad (3.23)$$

Variables from Equation 3.10 to Equation 3.17 were used in the same way. Two different algorithms were developed for the mathematical formulation of the pile group. One of them is for free-head pile groups, as considered by İşbuğa (2023). The other one is for pile groups which have rigid pile caps. In a rigid pile cap situation, all piles in a

group show the same top displacement but support different loads because of interaction, and in a free-head situation, a pile can show different displacements under the same load because of interaction.

3.6.1. Algorithm for Analysis of Free-Head Pile Groups

This section summarizes the algorithm used for the pile groups with free head conditions, which denotes that piles are loaded with force at the top surface rather than stringent displacement boundary conditions such as the rigid pile cap. The load acting on each pile in the group is defined as a point load on the top of the pile. Piles can have equal or different loads. As an example, point loads acting on piles in a pile group are shown in Figure 3.8. If the pile loads are the same, the displacements created by the pile under that load in the surrounding soil are calculated, and since it will be the same for other piles, the displacement in the soil is assigned to other piles and the interaction calculation is completed. This case makes the algorithm faster than the analysis under different loads. When the loads they exposed have different magnitudes for each pile, the displacements they create around the surrounding soil will be different for each pile, and in this case, the algorithm must repeat this step as many as the number of piles.

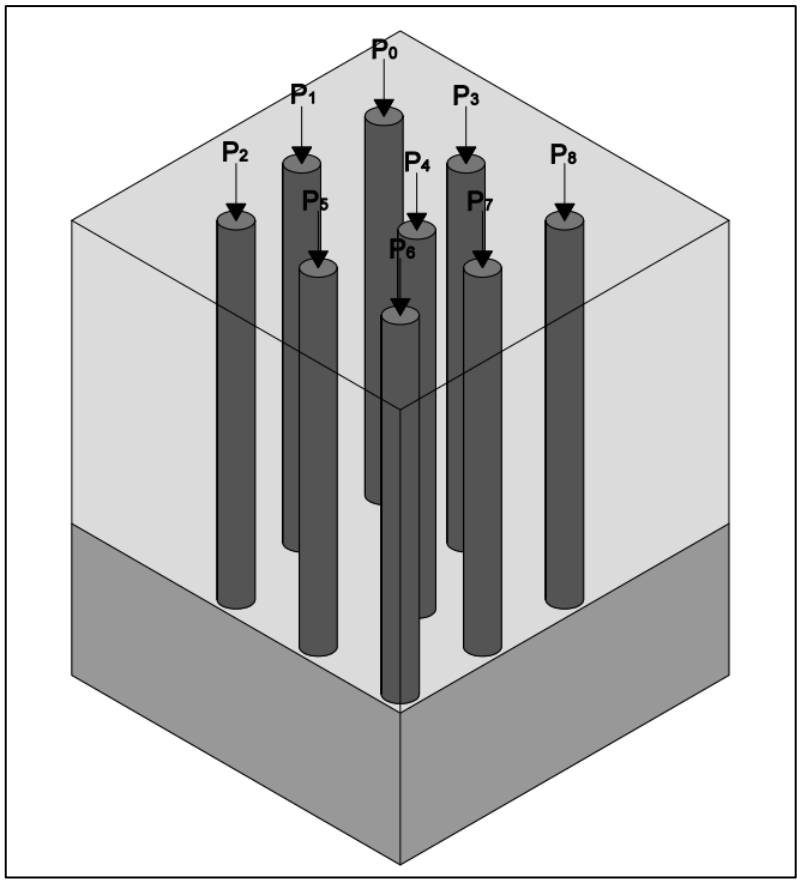

Figure 3.8 Point loads on piles

The input parameters we need to define in the program are as follows:

E_1: Elasticity of soil upper layer

E_2: Elasticity of soil bottom layer

E_p: Elasticity of piles

v_p: Poisson's ratio of piles

v_1: Poisson's ratio of upper soil

v_2: Poisson's ratio of bottom soil

P: Force acting on the piles

R: Radius of piles

l: Length of piles

N_Pile: number of piles

Coor: Coordinates of piles

dr: Radical increment for numerical derivation

dz: Vertical increment for numerical derivation

r: Length of the radial boundary of the model

err: Tolerable error

When deciding on vertical increment and radial increment of numerical differentiation, different values were used for analysis to test optimum incremental step size and the largest case where further minimization does not affect the result and is also below the acceptable error should be selected. Also, different values can be selected when deciding on the radial limit, but the smallest case should be chosen where increasing the limit more does not affect the interaction and displacement of piles.

The parameters that the algorithm calculates and uses as a result of the operations are as follows:

$\overline{E_1}$: Elasticity of soil upper layer in Vallabhan and Mustafa (1996)

$\overline{E_2}$: Elasticity of soil bottom layer in Vallabhan and Mustafa (1996)

G_1: Shear modulus of soil upper layer

G_2: Shear modulus of soil bottom layer

k_1: Stiffness parameters of Vallabhan and Mustafa (1996) for the upper soil layer

k_2: Stiffness parameters of Vallabhan and Mustafa (1996) for the bottom soil layer

t_1: Stiffness parameters of Vallabhan and Mustafa (1996) for the upper soil layer

t_2: Stiffness parameters of Vallabhan and Mustafa (1996) for the bottom soil layer

m: Function of Vallabhan and Mustafa (1996)

n: Function of Vallabhan and Mustafa (1996)

α: Function of Vallabhan and Mustafa (1996)

w_s: Soil displacement

Finally, we get the pile displacements (w_r) as output. We can summarize the algorithm as follows:

- When we enter the input data, the algorithm first calculates the shear modulus and elasticity to be used in the model.
- Then using the while loop, the algorithm calculates the single pile displacement and the soil displacement due to the pile. To begin this calculation, the algorithm must use Bessel's equation of order zero. A random value is assigned to start the while loop. This while loop continues until the margin of error is below the specified tolerance level. As a result of the first part, we get the single pile displacement and the soil displacement.

- In order to find the distances of the piles to each other, the distance matrix, including the relative distance of piles to each other, is calculated for each pile. By using the distance matrix, the total soil displacement at each pile point is calculated. After the nested loop in which the distance matrix is calculated, the displacements resulting from the interaction are found for each pile.

The flow chart of the algorithm is shown in Figure 3.9.

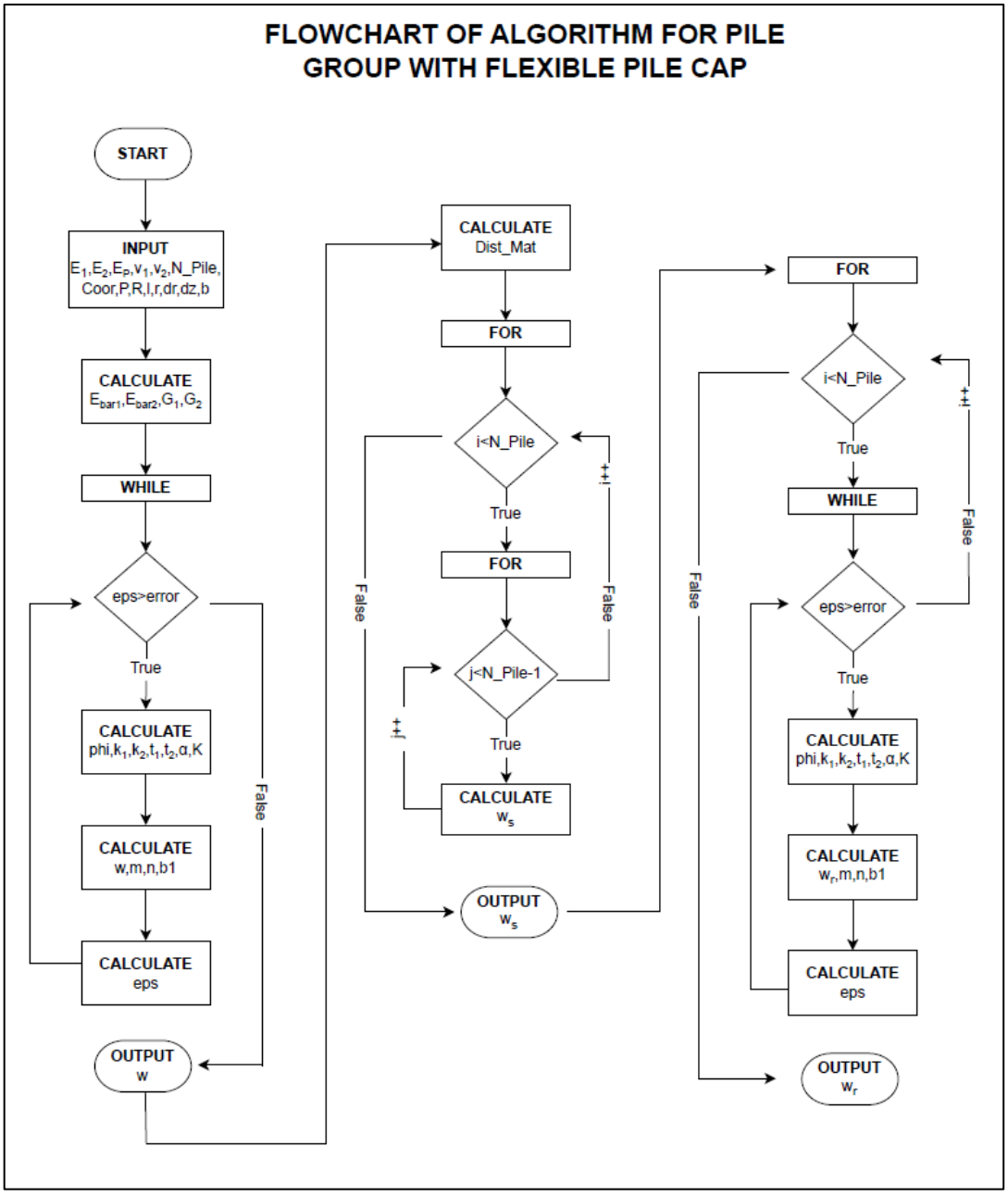

Figure 3.9 Flowchart of an algorithm for free head pile group

3.6.2. Algorithm for Analysis of Pile Groups with Rigid Pile Cap

In this situation, all piles in a group show the same displacement because of the rigidity of the pile cap. While having the same displacement at the top, the load taken by each pile is different because they are exposed to additional interaction forces, which will depend on the pile's location in the group. The additional settlements that the interaction forces would cause will be equaled by the rigid pile cap, which, in turn, compels the force distribution among the piles to be adjusted to comply with the same displacement at the top as a boundary condition.

In the scenario where the piles feature a rigid pile cap, the algorithm utilized for the analysis of free-head pile groups is initially employed. The displacement of piles in a group is calculated by applying a unit load to each pile using the algorithm of a free-head pile group situation. This unit load is applied to each pile separately so that the coefficients of that pile are found in the stiffness matrix for each loading. This step is applied to each pile within the group. Upon completing this loop for all piles, the stiffness matrix of the entire pile group, effectively representing the model, is obtained. Once we have the stiffness matrix, we can calculate the corresponding forces shown in Equation 3.24 by providing the displacement values as input.

$$[K]_{nxn} * [W]_n = [P]_n \tag{3.24}$$

where K is the stiffness matrix, W is the displacement matrix of the top displacement of piles, and P is the force matrix on piles.

In the case of a rigid pile cap, the algorithm performs more operations. First of all, we apply a unit load to each pile and calculate the top displacements corresponding to this unit load. Then, this operation is performed once in the case of a free-head pile group for each pile. In order to obtain the stiffness matrix, each pile must be loaded separately and the effect of the loaded pile on the other unloaded piles must be calculated. The coefficients in the row of the loaded pile in the stiffness matrix can be calculated. To create the stiffness matrix, the coefficients in the stiffness matrix of each pile are brought together and the matrix is created. After the stiffness matrix is created, the desired top displacement is given, and that displacement is assigned to each pile. Then, the load each pile carries under the same displacement is calculated. We know that the stiffness matrix of the system does not change with the load applied to the piles, the stiffness matrix

changes depending on the soil properties, pile properties, and the location of the piles. In these processes, we do not change the pile length, pile properties, soil properties, or pile layout, we only change the load on the piles. Equation 3.25 is obtained by multiplying Equation 3.24 with the inverse of the stiffness matrix.

$$[W]_n = [K]^{-1}{}_{nxn} * [P]_n \tag{3.25}$$

To use Equation 3.25, as we mentioned before, we loaded each pile separately and calculated the effect of this loading on the piles. Now, we will look at how the inverse of the stiffness matrix is calculated. To solve Equation 3.25, we load each pile separately, knowing that the stiffness matrix will not change with the load. We know that only one pile is loaded, and other piles are unloaded. Therefore, their values are zero in force matrix *P*. Inverse matrix of *K* is a matrix consisting of *k* elements, *W* is a matrix consisting of *w* elements, and *P* is a matrix consisting of *p* elements. Therefore, we can show this process in which we load the piles one by one as in Equation 3.26 below.

$$k_{i,j} = \frac{P_j}{w_i} \tag{3.26}$$

First, we loaded the first pile and obtained the displacement of the other piles according to this loading. By applying Equation 3.26, we find the first column of the inverse of the stiffness matrix.

$$k_{i,1} = \frac{P_1}{w_i} \tag{3.27}$$

When we load the first pile, we can use Equation 3.27. We know the *W* matrix so that we can find each element of the inverse of the stiffness matrix.

We repeat this process by loading the second pile, and when we load the second pile, we will find the second column of the inverse of the stiffness matrix. When this process is completed for each pile, we will have all the values of the inverse of the stiffness matrix. Since inverse of inverse of the stiffness matrix gives the stiffness matrix, we also find the stiffness matrix. In this way, we can now apply Equation 3.24.

After finding the stiffness matrix, we can now find the loads on the piles in the case of a rigid pile cap. In this case, since all piles will be displaced equally, we will give equal displacement to the piles and calculate the corresponding loads.

All piles are given equal displacement *w*. The corresponding loads were found by multiplying the stiffness matrix and the displacement matrix. On the right side of Equation 3.24 is the matrix with the corresponding loads.

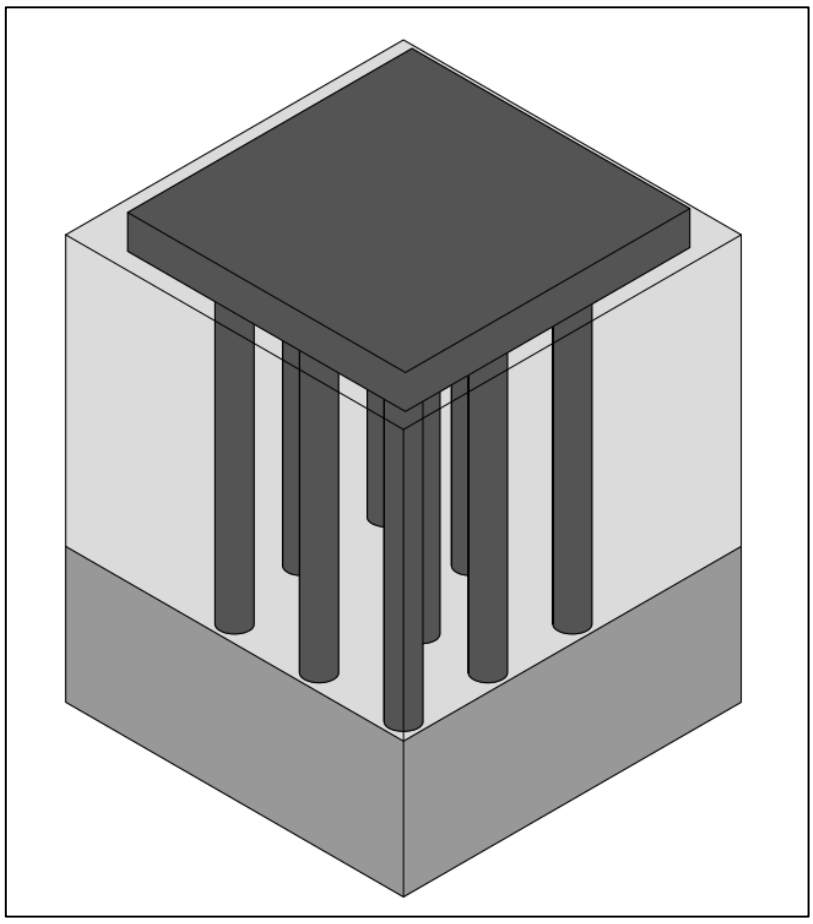

Figure 3.10 Pile group with rigid pile cap

Figure 3.10 shows the 3D view of a pile group consisting of nine piles with a rigid pile cap. In this case, the load is applied to the pile cap and all piles displace equally as a result of the stiffness of the pile cap. The flow chart of the algorithm is shown in Figure 3.11.

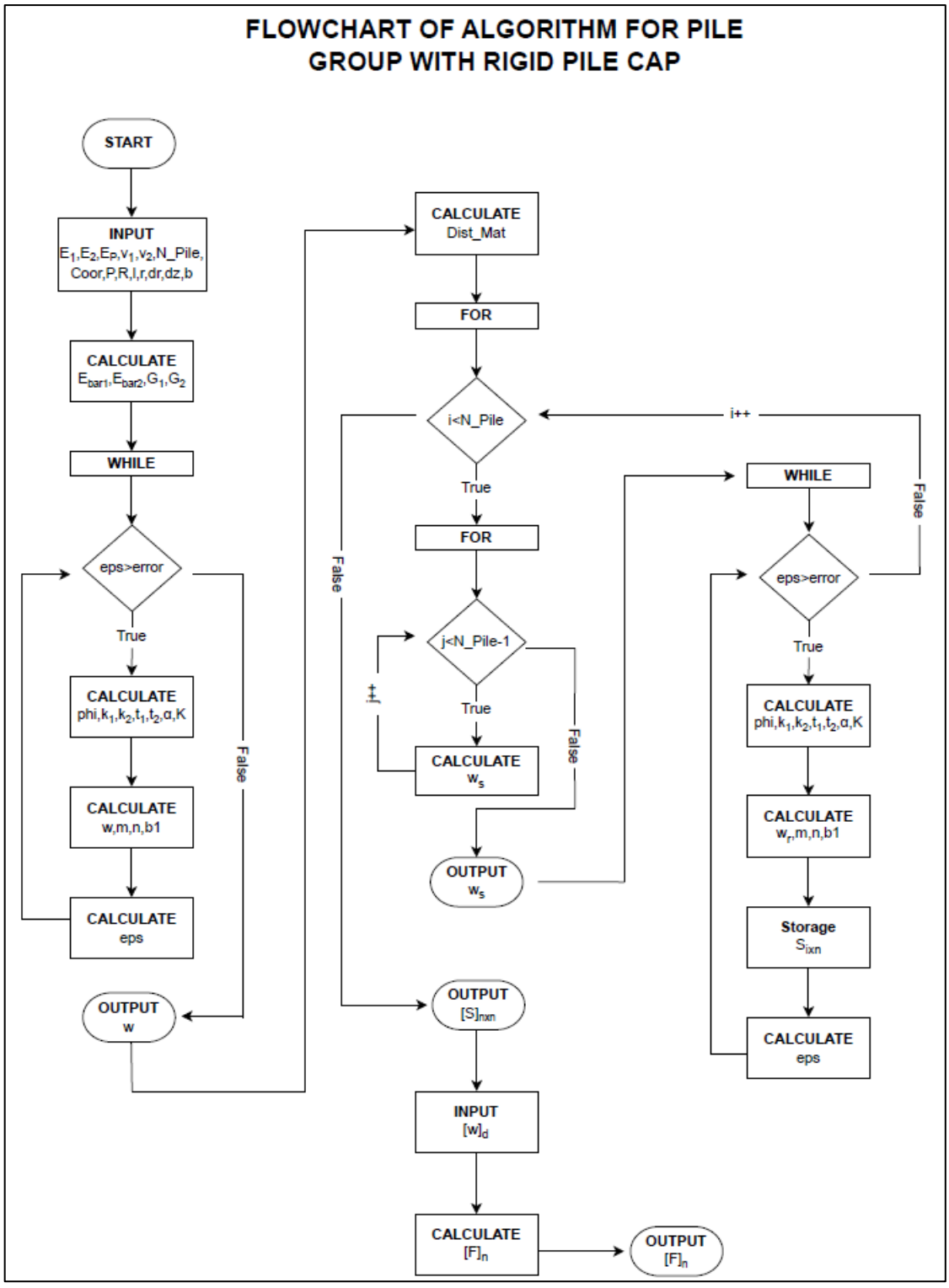

Figure 3.11 Flowchart of an algorithm for pile group with rigid pile cap

CHAPTER 4

RESULTS OF THE APPLICATION OF THE METHOD DEVELOPED FOR THIS STUDY

4.1. Introduction

In this chapter of the thesis results of the numerical analysis of the method which is used in this study are presented. Pile groups with different numbers of piles with different spacings are analyzed. Analyzed pile groups have rigid pile cap or they are free-head pile groups. Analysis results were compared with the results of the studies existing in the literature and those of the finite element methods.

4.2. Numerical Examples

The numerical results of pile groups analyzed in this study are given in this section. Four different cases were analyzed, including two free-head pile groups and two pile groups having rigid pile cap.

4.2.1. Example-1: Free Head Pile Group (3x1)

This section presents the application results of the algorithm, which is mentioned in Section 3.6.1, and compares the present study results with those of the finite element methods that were performed by using Abaqus. Abaqus is a suite of engineering analysis software packages. It is used for simulating the physical behavior of structures and solid bodies in response to a variety of factors, such as mechanical loads, temperature variations, contact interactions, impacts, and other environmental conditions (Simulia, 2008). Abaqus is primarily used for performing finite element analysis, a numerical simulation technique used to analyze the behavior of structures and systems under various conditions and loads. Abaqus was used for pile group analysis to compare the results of this study for comparison purposes. For this comparison, a pile group consisting of three (3x1) piles was analyzed. The interaction factor was determined for the results obtained

by increasing the spacing of this pile group. Both the interaction factors on the piles and the computation time of the proposed method and finite element method were compared. The layout of the analyzed pile group is shown in Figure 4.1 and Figure 4.2.

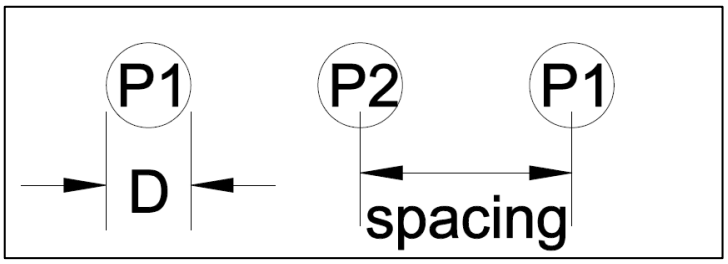

Figure 4.1 Plan view of 3x1 pile group

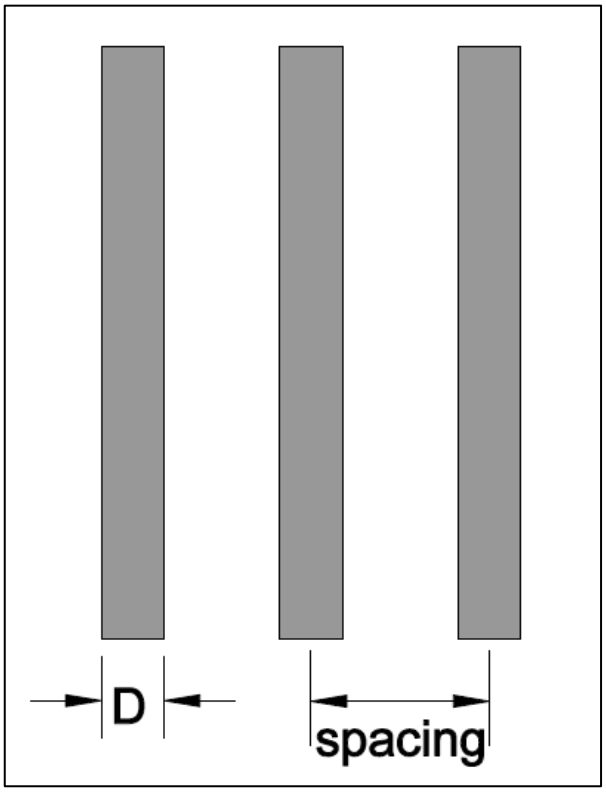

Figure 4.2 Section view of 3x1 pile group

The spacing between piles was increased step by step, starting from 2D up to 30D. The interaction factor-spacing graph was drawn with the results.

A pile with a diameter of 60 centimeters and a length of 30 meters was created as the soil domain in Abaqus. Properties of soil and pile are shown in Table 4.1.

Table 4.1 Properties of soil and pile

E_{soil}	10^3	kN/m^2
v_{soil}	0.3	-
E_{pile}	10^6	kN/m^2
v_{pile}	0.2	-
L_{pile}	15	m
D_{pile}	0.5	m

Boundary conditions of the soil domain are different at the sides and bottom of the soil. Displacement and rotations are used as boundary conditions in this analysis. Information about boundary conditions is given in Table 4.2 and Table 4.3.

Table 4.2 Boundary conditions on the side of the soil domain

Boundary Condition	Allowable (Yes/No)
Displacement in x-direction	No
Displacement in y-direction	No
Displacement in z-direction	No
Rotation in the x-direction	Yes
Rotation in the y-direction	Yes
Rotation in the z-direction	Yes

Table 4.3 Boundary conditions at the bottom of the soil domain

Boundary Condition	Allowable (Yes/No)
Displacement in x-direction	No
Displacement in y-direction	No
Displacement in z-direction	No
Rotation in the x-direction	No
Rotation in the y-direction	No
Rotation in the z-direction	No

As seen in Table 4.2, rotations were allowed at the side, but displacement was not. For the bottom of the soil domain displacement and rotations were not allowed.

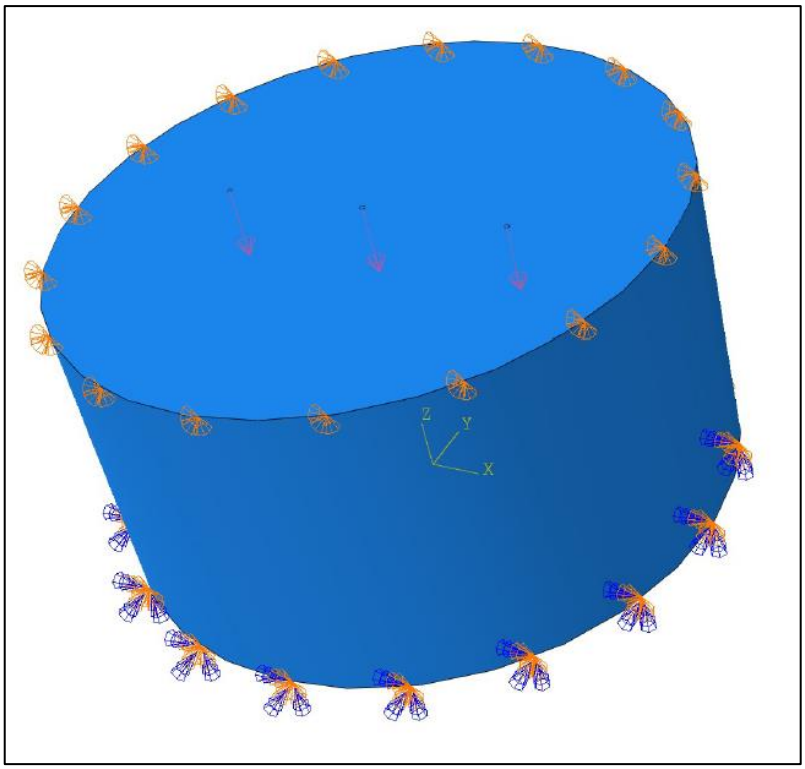

Figure 4.3 Boundary conditions and loads of model in Abaqus.

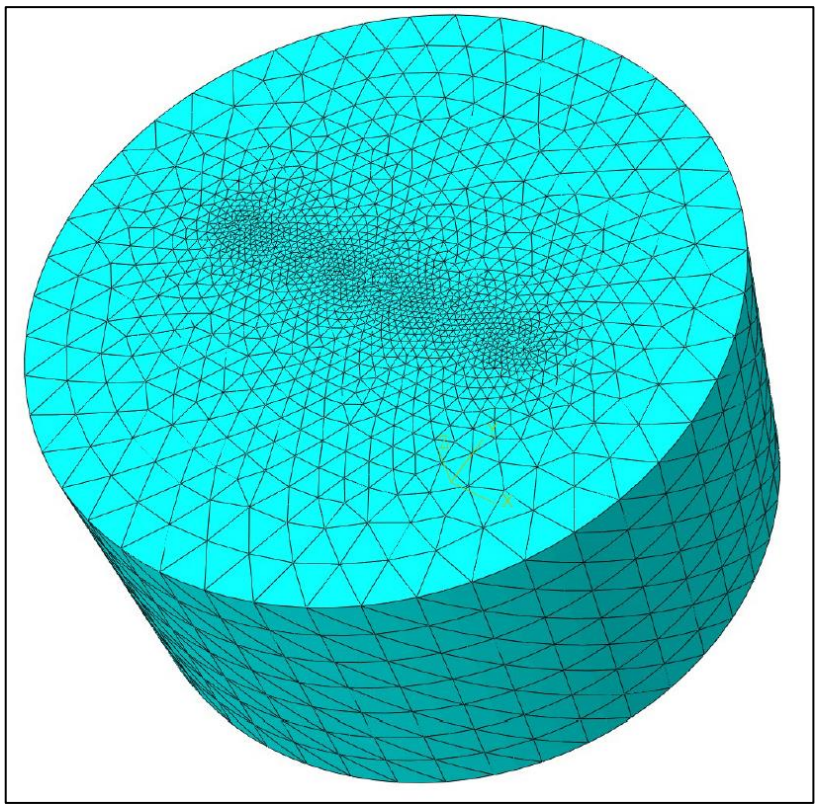

Figure 4.4 Mesh of finite element analysis when spacing is 30D.

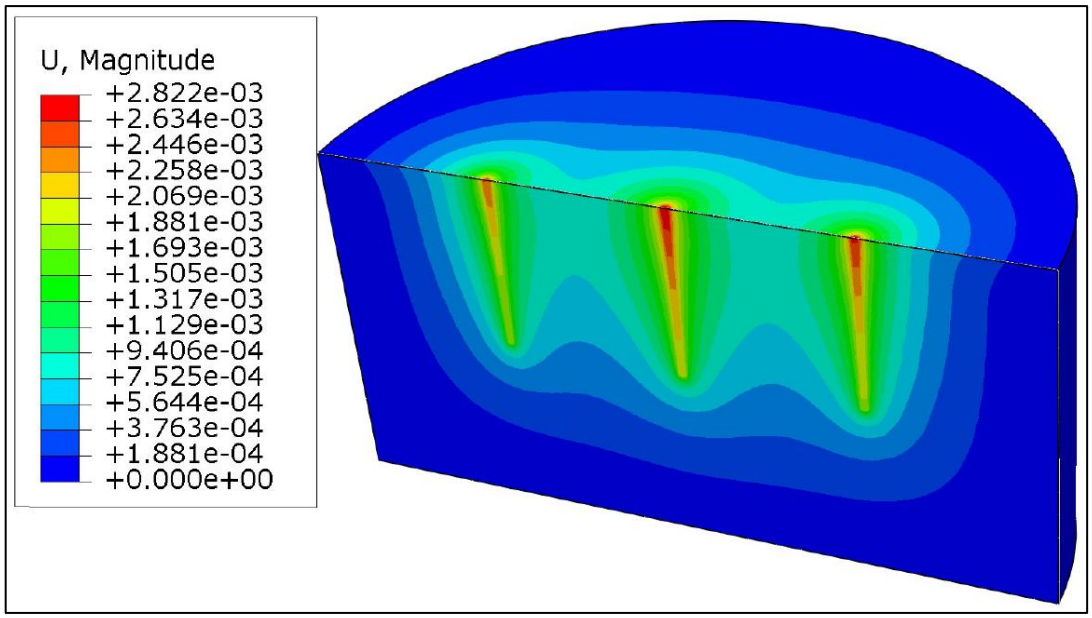

Figure 4.5 Results of finite element analysis in meter when spacing is 30D.

Figure 4.5 shows the results of finite element analysis when spacing is 30D. Generated mesh is also shown in Figure 4.4, triangular elements are used to form mesh and mesh is getting finer around the piles.

The results of the interaction factor of pile P2 are shown in Figure 4.6, P2 is the pile in the middle of the other two piles.

Poulos (1968) calculated the interaction factor by subtracting the displacement of a single pile carrying the same load from the displacement of piles within the group and dividing the result by the displacement of a single pile. For example, the interaction factor for the P2 pile was calculated as in equation 4.1, α is the interaction factor.

$$\alpha = \left(w_{P2} - w_{single}\right)/w_{single} \tag{4.1}$$

Where w_{single} is the single pile top displacement under identical conditions and w_{P2} is the top displacement of pile P2. The interaction factor was calculated for each spacing by changing the spacing between piles and the interaction factor vs. s/D plot, where *s* is the spacing, is shown in Figure 4.6.

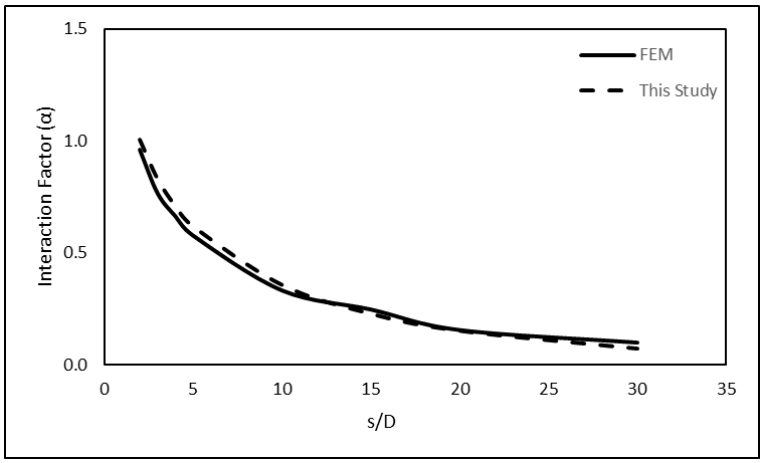

Figure 4.6 Interaction factor vs. s/D graph for the pile P2.

The interaction factor vs. s/D plot is also drawn for the P1 pile and is shown in Figure 4.7.

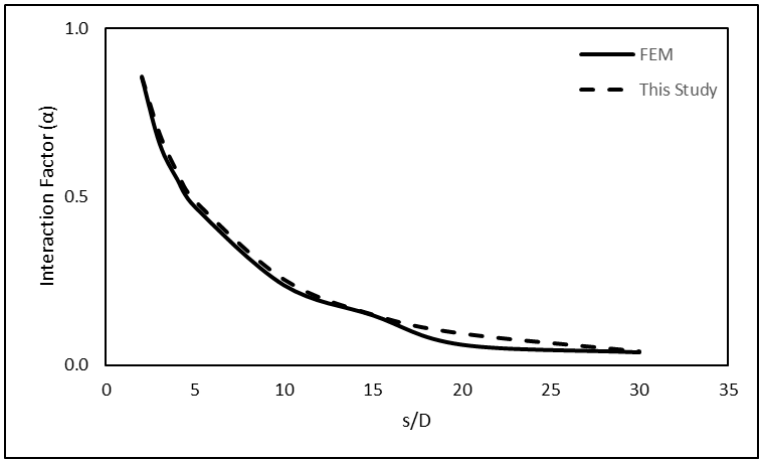

Figure 4.7 Interaction factor vs. s/D graph for the pile P1.

The presence of a strong agreement between the finite element method and this study in terms of interaction factors, as demonstrated in Figure 4.6 and Figure 4.7, is clearly observable. This matching result suggests that the method proposed in this study aligns well with the finite element method, strengthening the credibility of the current study.

Comparing the solution times of the finite element method and the study is a valuable way to assess the computational efficiency of each method. Additionally, considering the number of nodes in the mesh for both the model proposed in this study and the finite element method is essential, as it can provide insights into the computational complexity of the models and their ability to handle the analysis efficiently. The number

of nodes in the mesh created in the models and the computation times of these models are given in Table 4.4.

Table 4.4 Computational time and node number of FEM and This Study

	FEM		This Study	
Spacing	Number of Nodes	Time (s)	Number of Nodes	Time (s)
2D	71070	59.00	300000	1.22
3D	24910	20.00	300000	1.28
4D	23700	20.00	300000	1.14
5D	21722	18.00	300000	1.20
10D	25128	22.00	300000	1.12
15D	141015	165.00	300000	1.12
20D	134405	129.00	300000	1.19
30D	94176	94.00	300000	1.17

The significant difference in solution times between this study and the finite element method, as demonstrated in Table 4.4, is remarkable. It's apparent that this study achieves solutions much faster, so this can have practical implications for efficiency and productivity in engineering and analysis tasks.

The comparison of displacements at the top of the P2 pile between the finite element models and this study, as shown in Figure 4.8, indicates a difference of approximately 10%. The results of this study are around 10% smaller than those obtained from finite element analysis. This difference can be attributed to the fact that this study does not account for the radial displacement in the model.

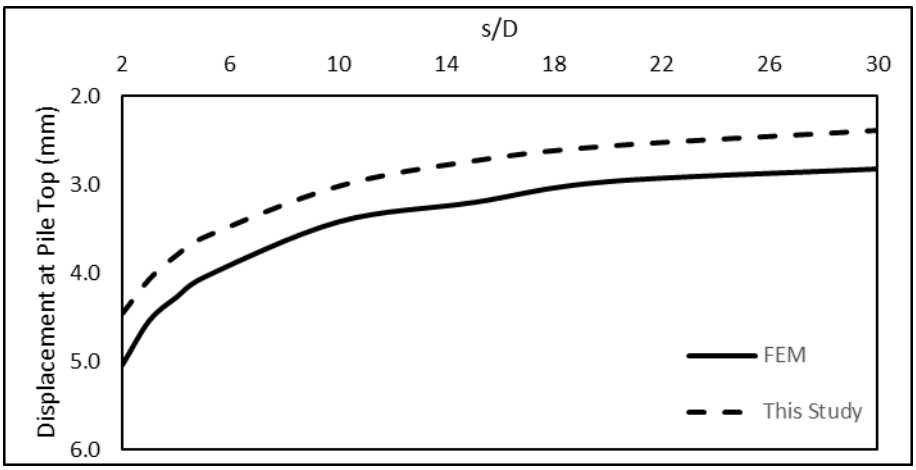

Figure 4.8 Displacement at the pile top (P2) vs. s/D

It's noteworthy that the 10% difference appears to be consistent across different pile spacings. This consistency suggests that the mesh used in the study doesn't significantly affect the results. Rather, the primary reason for the difference lies in the fact that radial displacement is not considered in the study, which is inherited from the single pile model used as a basis for this study. If radial displacement was allowed in this study, it might have influenced the results, likely leading to increased pile displacements.

4.2.2. Example-2: Free Head Pile Group (5 Pile)

In this section, a pile group consisting of five piles was analyzed with the Abaqus software and the methods developed in this study. The plan view of the model is given in Figure 4.9. As it can be seen in Figure 4.9, there are piles in the corners and one in the middle. Since the piles at the corners will behave symmetrically under equal loads, the same numbering is used for them. In this model, the pile that will show different displacements under equal load is the one in the middle.

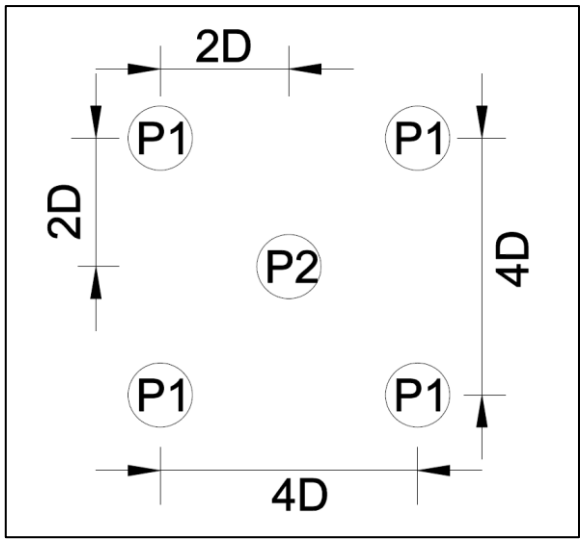

Figure 4.9 Plan view of pile group

The soil properties are shown in Figure 4.10, three different soils can be seen. This problem is also modeled in finite element method. However, the model written in this study is suitable for two-layered soils. In the proposed model, it is possible to model soil along the pile depth and a different soil below the pile toe. For this reason, the soil shown in Figure 4.10 was used for the bottom of the pile, but the weighted average of the soils shown in Figure 4.10 was taken for the soil around the pile.

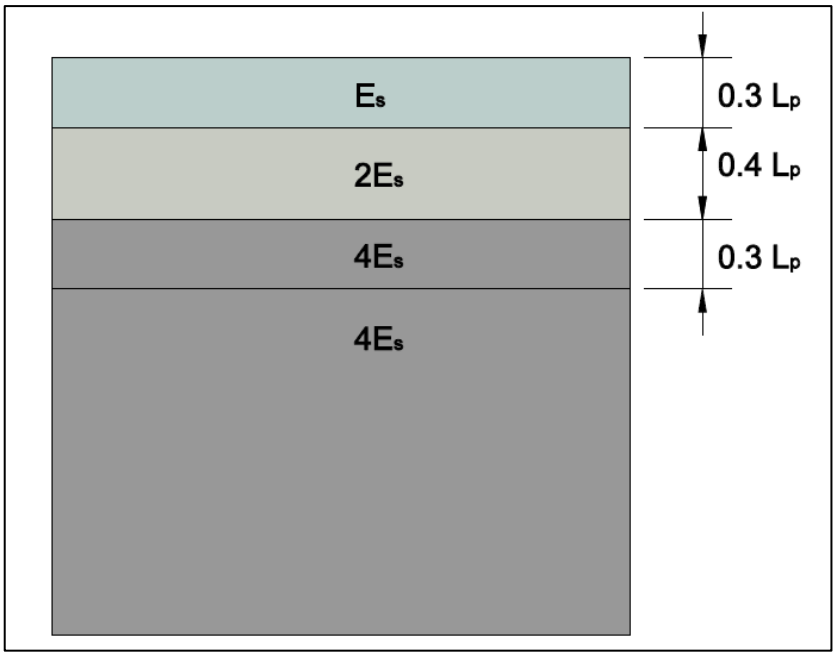

Figure 4.10 Soil properties of the FEM model

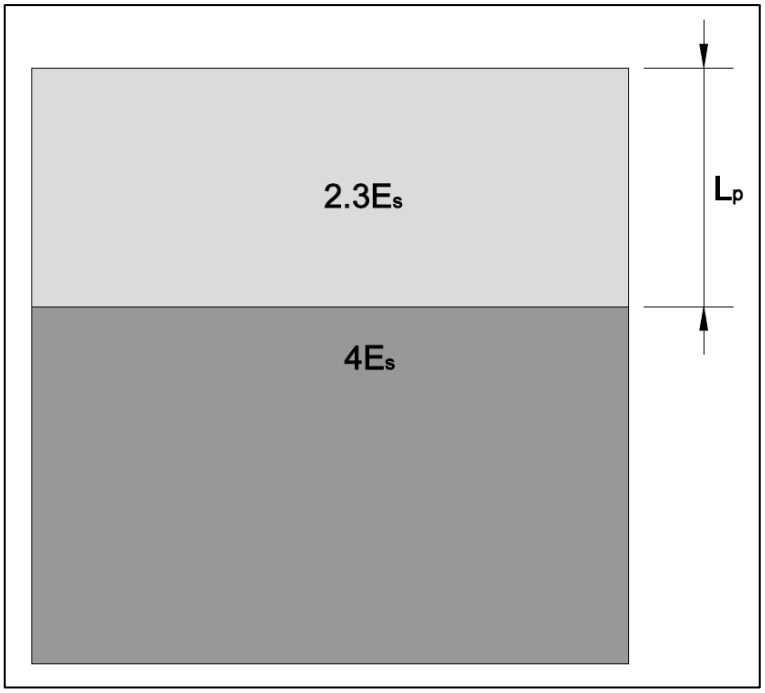

Figure 4.11 Averaged soil properties used for the current study

Three-dimensional views of the models are shown in Figure 4.12 and Figure 4.13. As seen in Figure 4.12, three different soil types were applied around the piles in finite element analysis. For the model proposed in this study, there are two soil layers one of them around the piles and the other one below the pile toe as seen in Figure 4.13.

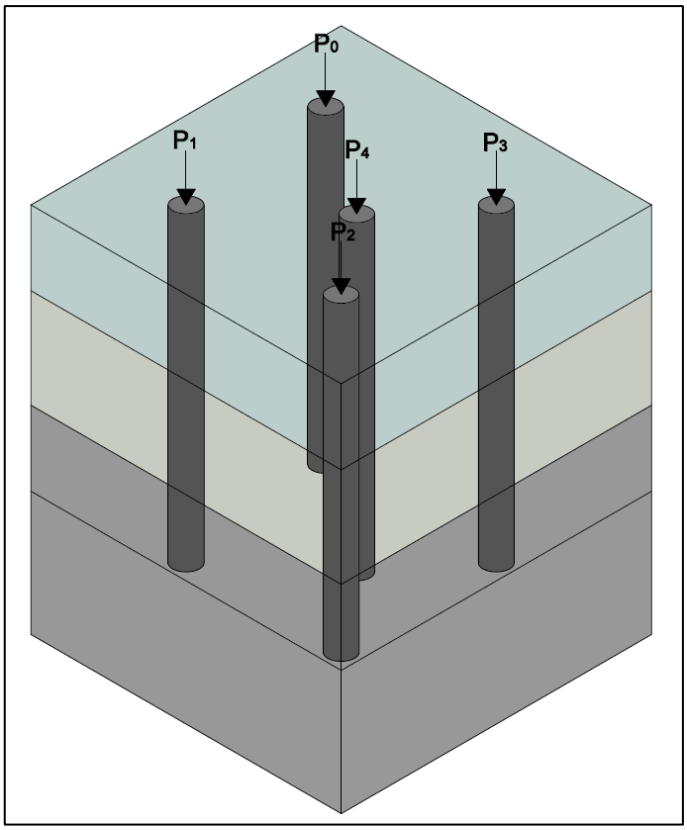

Figure 4.12 3D view of the FEM model

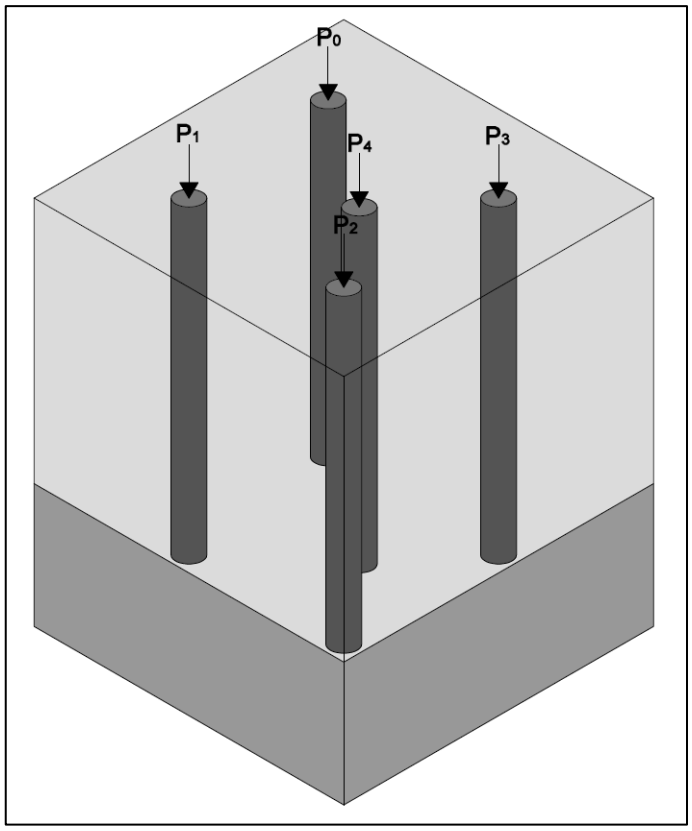

Figure 4.13 3D view of the current study model

The soil and pile properties used in this analysis are given in Table 4.5. It was multiplied by the coefficient numbers given in Figure 4.10 and Figure 4.11 and used in the models.

Table 4.5 Properties of soil and pile

E_{soil}	10^3	kN/m^2
v_{soil}	0.3	-
E_{pile}	10^6	kN/m^2
v_{pile}	0.2	-
L_{pile}	14	m
D_{pile}	0.5	m

The boundary conditions used in the finite element model are the same as the boundary conditions given in Table 4.2 and Table 4.3. The view of boundary conditions in the finite element model is shown in Figure 4.14.

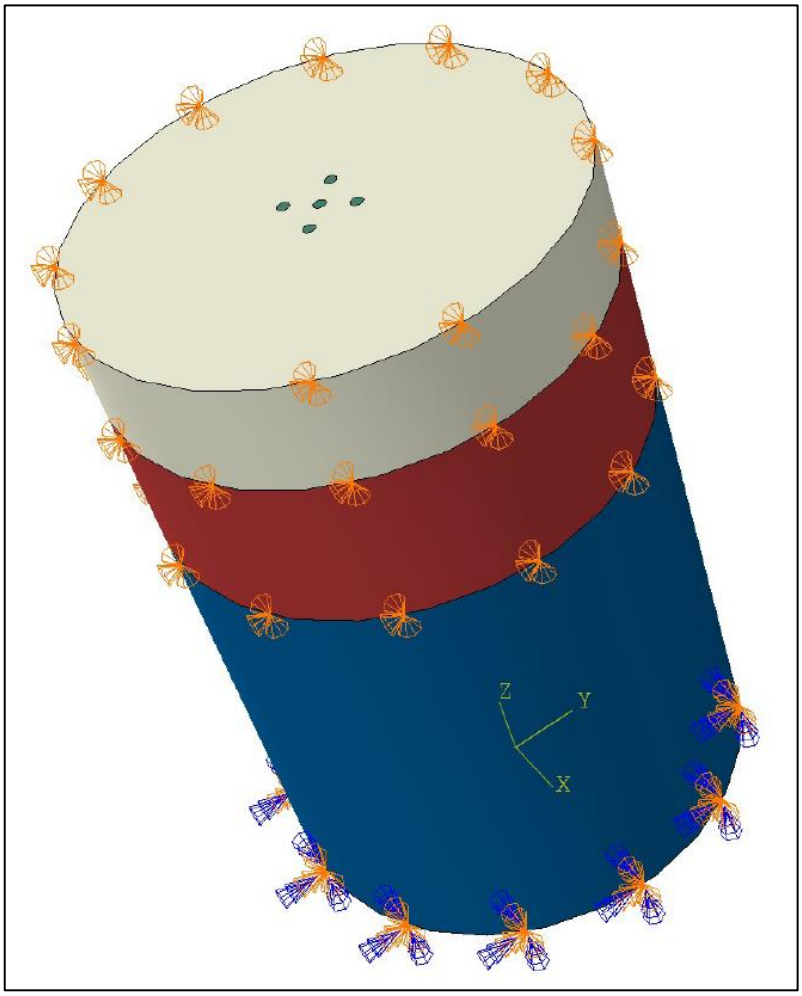

Figure 4.14 Boundary conditions of the model in Abaqus.

Each of the five piles in the model carries a load of 100 kPa. The load is given as surface traction in finite element analysis. However, in the proposed method, the load is given as point load and each pile is loaded with 19.64 kN point load, this value is obtained by multiplying 100 kPa by the pile surface area. The mesh used in finite element analysis is shown in Figure 4.15, there are a total of 316252 nodes in this mesh.

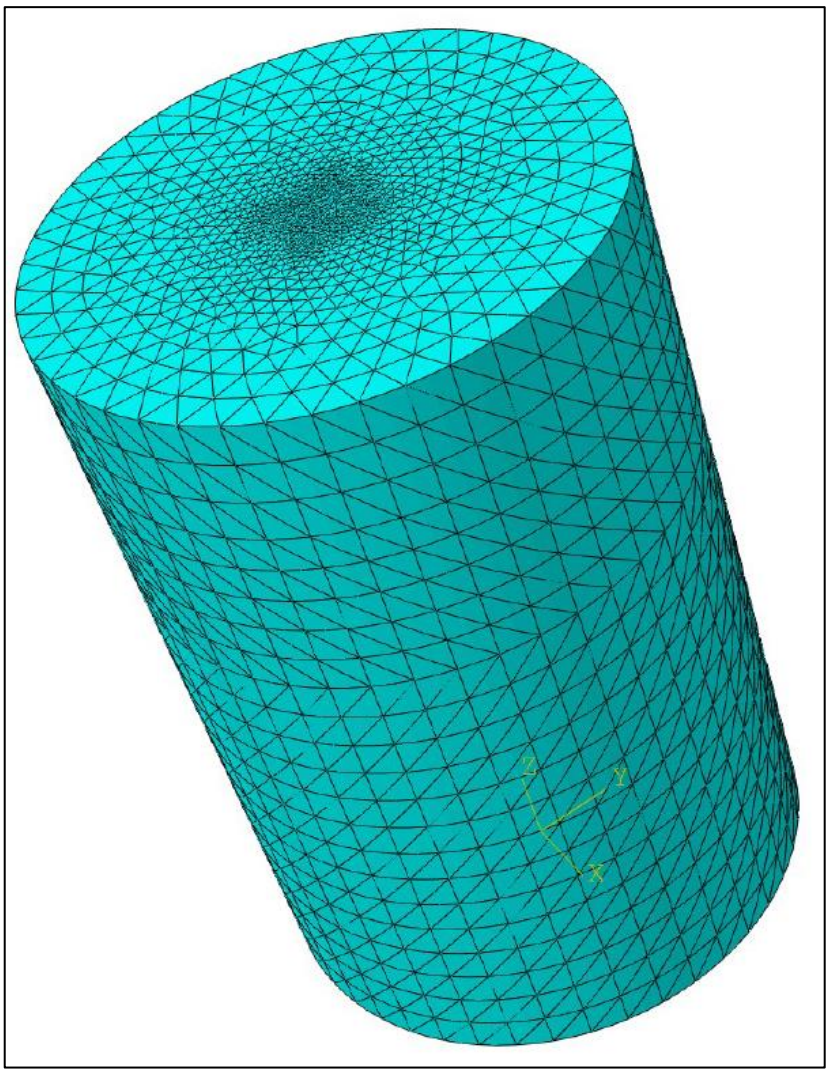

Figure 4.15 Mesh of finite element model.

Finite element analysis results are shown in cross-section in Figure 4.16. The section taken cuts the middle pile from its center.

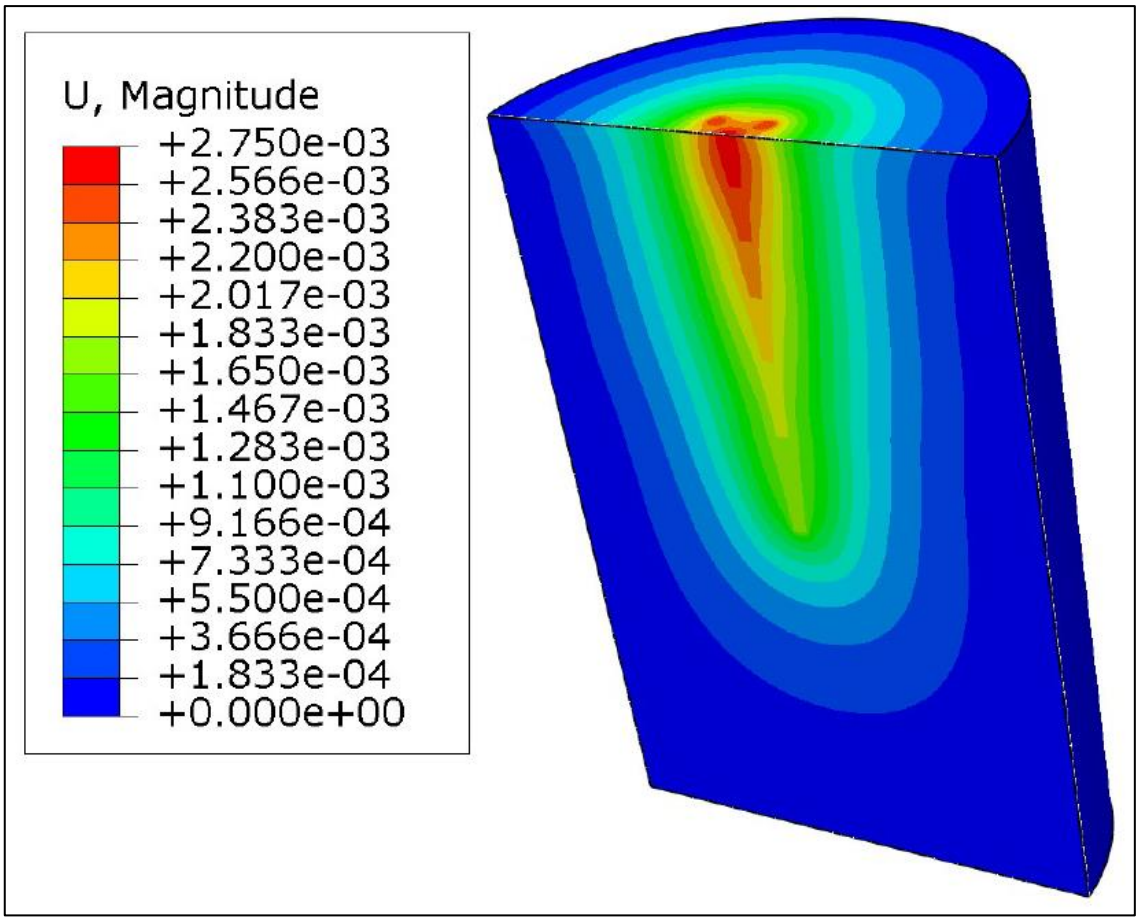

Figure 4.16 Results of finite element analysis.

In Figure 4.16, the model results are shown with contours. The section cuts the middle pile from its center. The two piles behind the center pile can also be seen in this section.

In the layout shown in Figure 4.9, the pile expected to show the most displacement is the pile in the center. The pile in the center is the pile closest to all the other piles, and thus it is the pile that interacts with the other piles the most. For this reason, the results of the finite element method and those of this study were compared for the center pile. This comparison aims to measure the success of this study against the finite element method in modeling the interaction between piles.

In Figure 4.17, the finite element method results and the results found with the current study are compared.

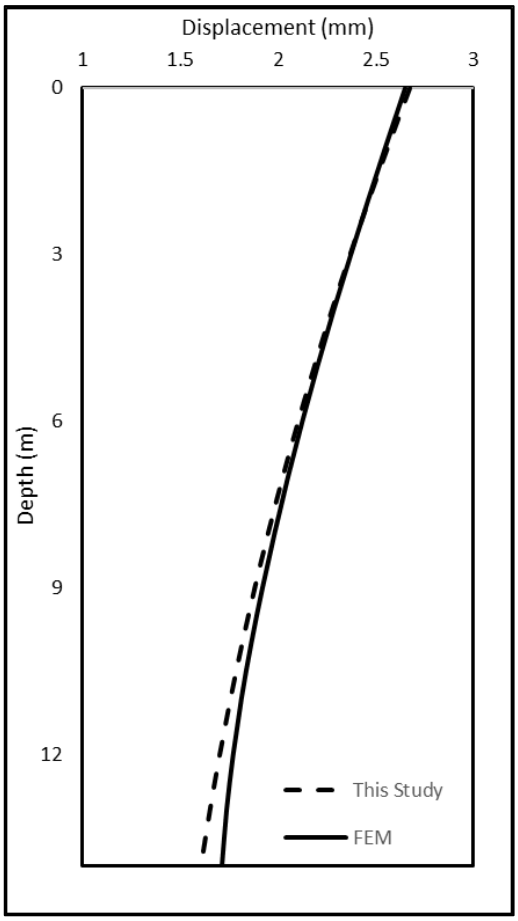

Figure 4.17 Displacement of the center pile along its depth in FEM and this study

As seen in Figure 4.17, the results of the current study are compatible with finite element method. The computation time of the finite element method and the current study are presented in Table 4.6.

Table 4.6 Computational time and node number of FEM and This Study

FEM		This Study	
Number of Nodes	Time (s)	Number of Nodes	Time (s)
316252	871.80	280000	1.39

As can be seen in Table 4.6, the computation time of the current study in reaching the solution is much faster than the finite element method.

4.2.3. Example-3: Pile Group with Rigid Pile Cap (3 x 3)

Chen et al. (2011) conducted an analysis of pile groups using their unique model, which is detailed in Section 2.3.5. They specifically studied a 3x3 pile group with a rigid pile cap and compared the forces supported by the single piles within the group.

The layout of the pile group is illustrated in Figure 4.18 and Figure 4.19. Notably, there are three distinct types of piles due to their positions within the layout. Corner piles are situated at the corners of the layout and exhibit symmetrical behavior relative to one another. Side piles are positioned along the sides of the layout and demonstrate symmetrical behavior among themselves. Centre pile is one pile situated in the center of the layout.

The analysis focused on understanding how these different pile positions and their symmetrical or asymmetrical arrangements within the group influence the distribution of forces and load-sharing characteristics among the piles.

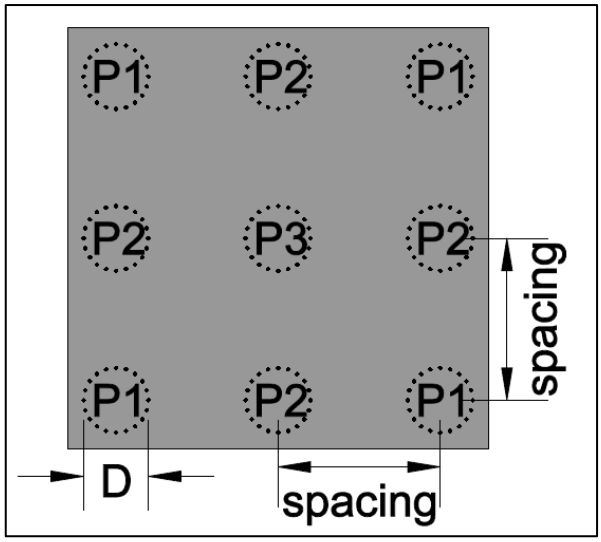

Figure 4.18 Plan view of 3x3 pile group

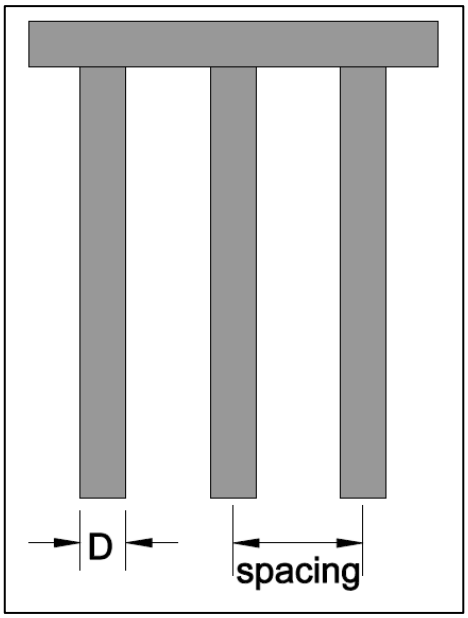

Figure 4.19 Section view of 3x3 pile group

Chen et al. (2011) used a ratio of L/D=60, indicating that the length of the pile (L) was 60 times greater than its diameter (D). This value characterizes the geometry of the piles within the group. The Poisson's ratio for the soil was set to 0.3. Poisson's ratio is a material property that describes how a material deforms in response to a load. In this case, it represents the soil's behavior. The researchers used two different E_p/E_s ratios, where E_p is Young's modulus of pile and E_s is the Young's modulus of soil.

The results of their analysis for these two different values of Young's modulus ratio are presented in Figure 4.20 and Figure 4.21. These figures illustrate how changes in the stiffness properties of the soil and pile materials impact the forces supported by the single piles within the group.

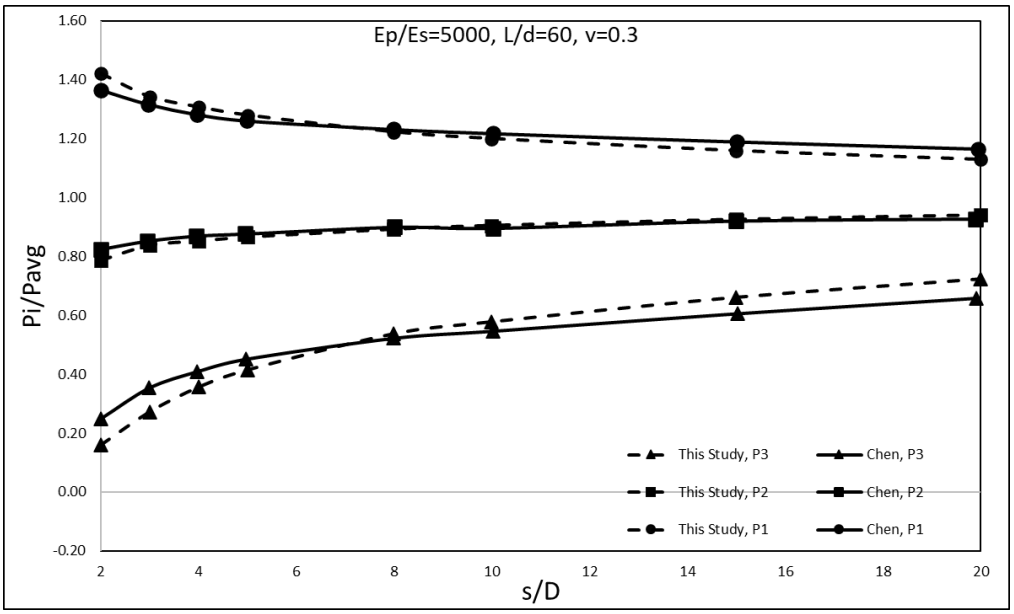

Figure 4.20 Spacing - load distribution graph of in 3x3 pile group: $E_p/E_s = 5000$

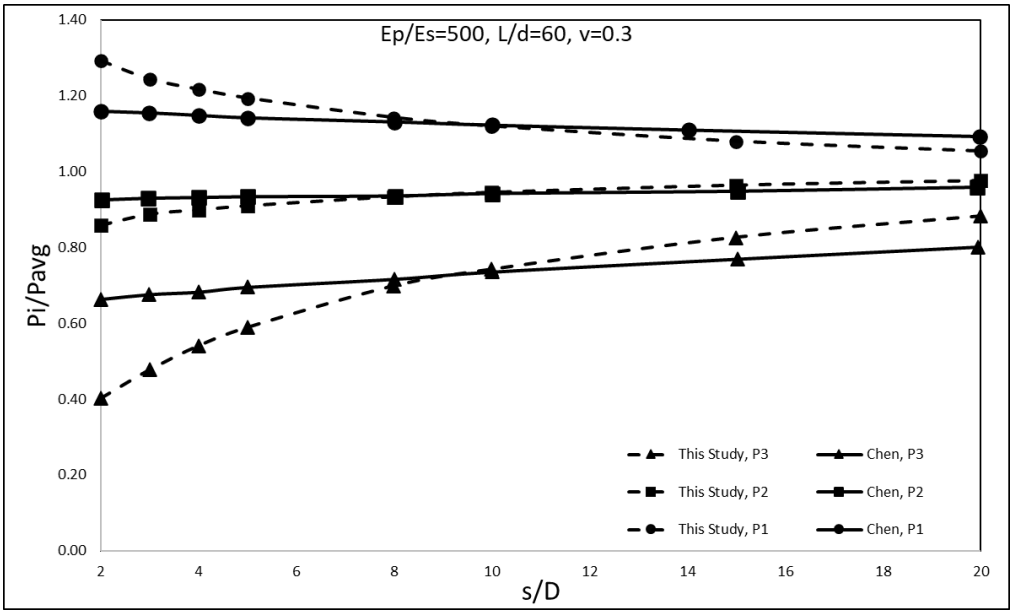

Figure 4.21 Spacing - load distribution graph of in 3x3 pile group: $E_p/E_s = 500$

In Figure 4.20, the results are in good agreement with the results of Chen et al. (2011). However, the difference between this study and Chen et al. (2011) increases as the ratio of Young's modulus (E_p/E_s) decreases as seen in Figure 4.21.

In this study, the interaction responds faster as the spacing between the piles increases, as the spacing increases, the piles reach to support the same load faster.

4.2.4. Example-4: Pile Group with Rigid Pile Cap (5 Pile)

In this section, the case of the model mentioned in Section 4.2.2 with a rigid pile cap is analyzed. This was analyzed by finite element method and the method developed in this study. The rigid pile cap case for finite element method was calculated using a similar method as in the approach mentioned in Section 3.6.2. For this, the stiffness matrix of the system was found by loading each pile separately in the finite element model. After finding the stiffness matrix, the forces on the piles were calculated by using the finite element results with the method in the algorithm described in Section 3.6.2. The results of this study were calculated using the algorithm described in Section 3.7.2 and used in Section 4.2.3. The plan view of the pile layout is given in Figure 4.22.

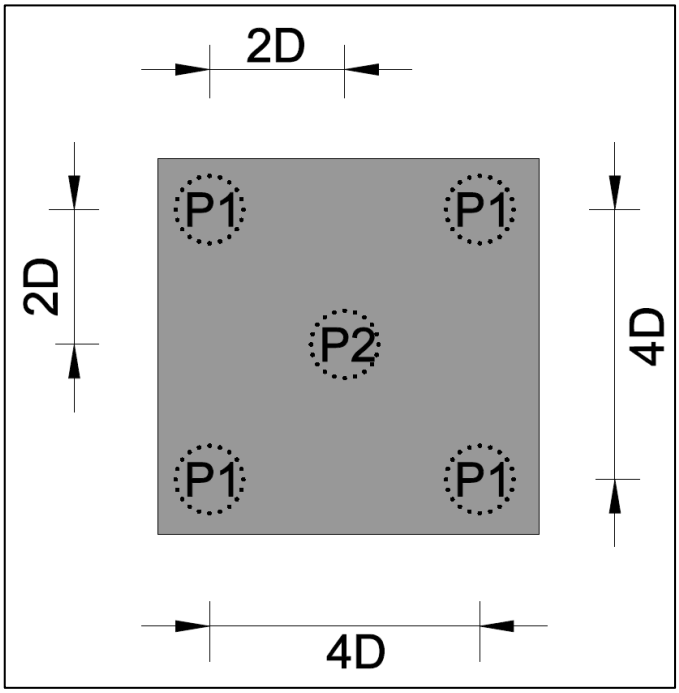

Figure 4.22 Plan view of pile group

In the finite element analysis, the soil shown in Figure 4.10 was modeled. For the proposed method, the soil shown in Figure 4.11 was modeled. As soil properties, the properties specified in Table 4.5 were used.

The three-dimensional view of the models used in the finite element method and the model performed in the current study are given in Figure 4.23 and Figure 4.24.

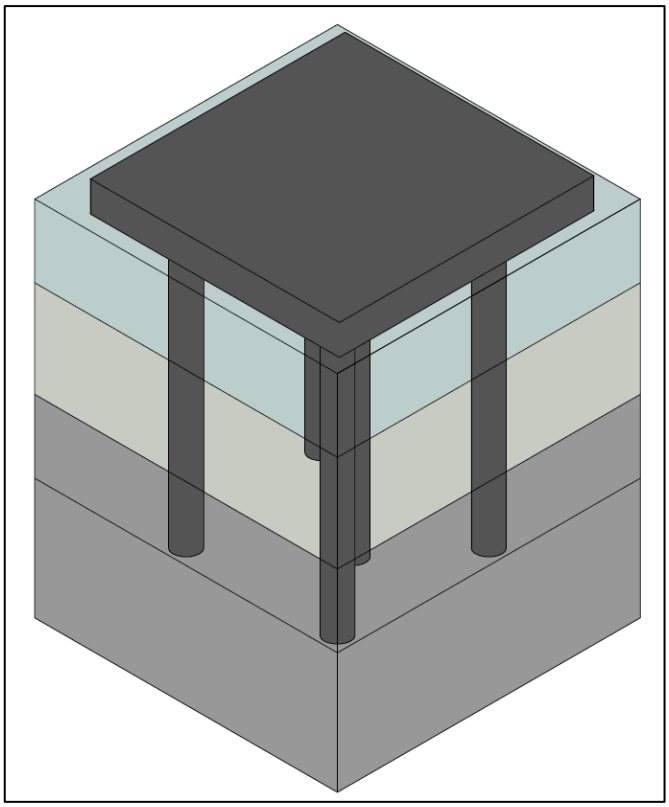

Figure 4.23 3D view of the FEM model

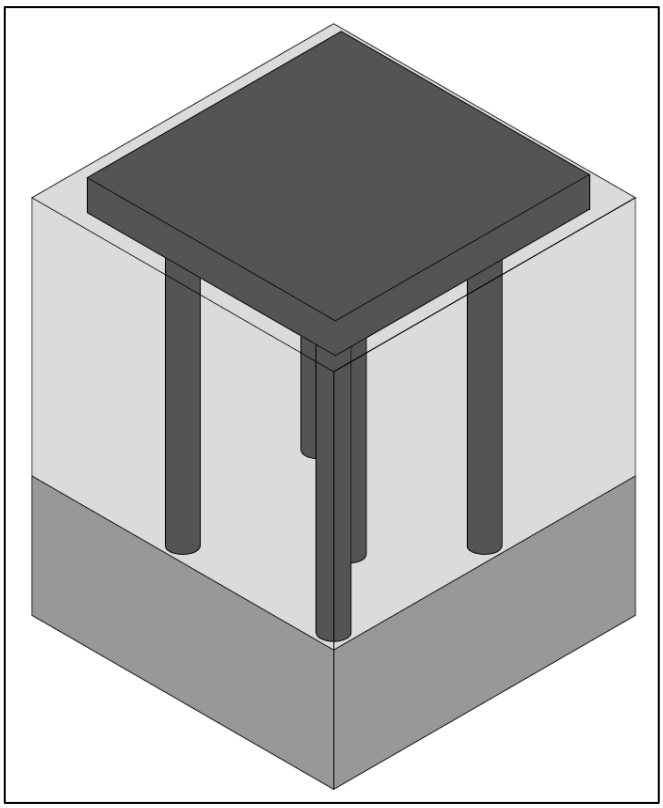

Figure 4.24 3D view of the current study model

Table 4.7 Results and computational times of FEM and This Study

FEM			This Study		
Number of Node	Time (s)	Pcenter/Pavg	Number of Node	Time (s)	Pcenter/Pavg
316252	955.00	0.75	280000	4.13	0.65

Looking at the results in Table 4.7, the computation time of the proposed method is smaller than that of the finite element method. In other words, in the result of the approach applied in this study, the pile in the center carries 65% of the average load per pile. However, according to the finite element method, the pile in the center carries 75% of the average load per pile. It is understood from these results that the approach used in this study finds the interaction between piles more than the finite element method. If there was no interaction between the piles, each of them would carry an equal load, but due to the interaction, the load carried by the pile in the center is less since it already shows displacement.

In the approach applied in this study, the stiffness created by the piles in the area where they are located is not taken into account. More precisely, in this approach, the area where the piles are located is taken into account as the soil and then the displacement in the soil is transferred to the pile located there. The finite element method, on the other hand, takes into account the stiffness of the pile in the soil. Therefore, in the finite element method, the pile in the center carries more load. The difference between the results is explained in this way.

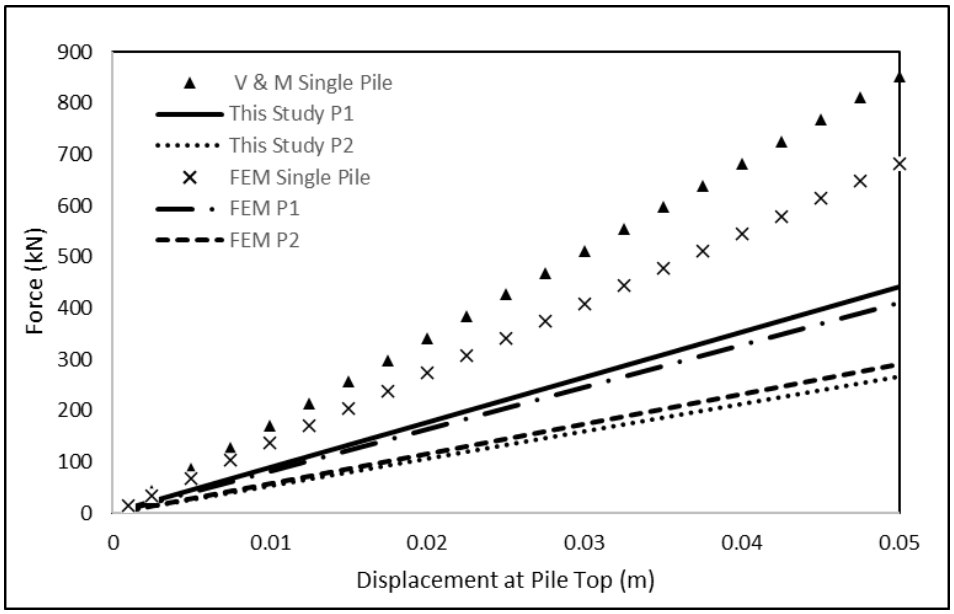

Figure 4.25 Load-Displacement curve of corner pile and center pile

The analyses were repeated under different loads using the proposed method. The load-displacement graphs for the corner piles and the center pile are shown in Figure 4.25.

As can be seen in Figure 4.25, the difference between the graphs increases as the load increases, but the ratio between them does not change. The center pile carries 65% of the average load per pile under each loading. This is expected because, in the model developed in this study, the soil and the pile are considered as elastic materials.

Figure 4.25 shows that in the finite element method, the difference between the loads carried by the piles in the group is less than those found in the current study. This is because, as mentioned earlier, the approach in this study does not take into account the stiffness of the piles on the soil. Instead, the location of the piles is considered as the soil, and the soil displacement due to the neighboring piles at that point is calculated, and the total soil displacement is converted to the interaction force by multiplying it with soil stiffness parameters. This interaction force acts on the receiver pile. When we look at the single pile results, we see that the results of this study are higher than those of the finite element method. However, in the group pile results (P2 pile), the results of this study have less load than the finite element method results. This shows that not taking stiffness which is caused by piles in the soil into account may cause us to overestimate the interaction between the piles.

CHAPTER 5

CONCLUSION

In this study, different pile groups were analyzed, and the analysis results were compared with previous studies and finite element method results. Cases, including pile groups that have rigid pile caps and no capping (free-head) are considered separately, and comparisons, including finite element method results and other existing methods in the literature, are made accordingly. In addition, analysis was made using a weighted average for non-homogeneous soils, and the results of this analysis were modeled as non-homogeneous in the finite element method, and a comparison was made between them.

In the case of the free head, the interaction factor calculated for the piles shows that the results are in good agreement with the finite element method. In the same results, there is a 10% difference in terms of displacements between the model developed in this study and the finite element method, and the finite element method results show more displacement. In terms of computation time, the model developed in this study is much faster than the finite element method.

The model developed in this study for non-homogeneous soil conditions is not suitable for direct use; currently, this model allows the defining of two soil layers. It is possible to model soil along the pile depth and a different soil below the pile toe. For this reason, soil parameters were used by taking the weighted average for the non-homogeneous situation. Analyses performed in this way have shown that the analyses made by taking the weighted average of elasticity moduli are in good agreement with the finite element method results. In this way, it can be said that this model developed can also be used for non-homogeneous cases.

The results of this study show that the developed model is more successful than the finite element method in terms of computation time. However, it is still possible to improve the model. From this perspective, the work to be done to develop the model can be listed as follows:

- Radial displacements are not taken into account in the model developed in this study, which may be one of the significant reasons for the difference in results.

- The model does not take into account the stiffness created by placing the piles in the soil; taking this situation into account will change the interaction between the piles.
- For non-homogeneous soils, analyses are made by taking a weighted average. This situation can be improved by making the model suitable for non-homogeneous soils.

This study shows us that the proposed model presents results that match those of the finite element method and the other models previously proposed by researchers in the literature. In addition, the proposed method reaches a solution many times faster than the finite element metod. For this reason, it is understood from the analysis results that the success of this model is undeniable.

REFERENCES

Aron, C., & Jonas, E. (2012). *Structural Element Approaches for.* Göteborg: CHALMERS UNIVERSITY OF TECHNOLOGY.

Bathe, K., & Wilson, E. (1976). Numerical Methods in Finite Element Analysis. *Englewood Cliffs*.

Butterfield, R., & Banerjee, P. K. (1971). The Elastic Analysis of Compressible Piles and Pile Groups. *Géotechnique, 21*(1), s. 43-60.

Byrne, P. M. (1991). A Cyclic Shear-Volume Coupling and Pore Pressure Model for. *Second international conference on recent advances in geotechnical earthquake engineering and soil dynamics*, (s. 11–15). St. Louis-Missouri.

Cao, M., & Chen, L.-z. (2008, 4). Analysis of interaction factors between two piles. *Journal of Shanghai Jiaotong University (Science), 13*(2), s. 171-176.

Chapra, S. C., & Canale, R. P. (2010). *Numerical Methods for Engineers* (6th Edition b.). New York: McGraw-Hill.

Chen, S. L., Song, C. Y., & Chen, L. Z. (2011). Two-pile interaction factor revisited. *Canadian Geotechnical Journal, 48*(5), s. 754-766.

Chow, Y. K. (1986, December). Discrete element analysis of settlement of pile groups. *Computers & Structures, 24*, s. 157-166.

Crispin, J., Leahy, C., & Mylonakis, G. (2018, December). Winkler Model for Axially-Loaded Piles in Inhomogeneous Soil. *Géotechnique Letters*, s. 1-25.

Cundall, P. A., Hansteen, H., Lacasse, S., & Selnes, P. (1980). *Soil Structure Interaction Program for Dynamic and Static Problems.* Norwegian Geotechnical Institute.

Das, B. M. (2016). *Principles of Foundation Engineering.* Cengage Learning.

Das, B. M. (2019). *Advanced Soil Mechanics.* Florida: CRC Press.

El Sharnouby, B., & Novak, M. (1986). Flexibility Coefficiient and Interaction Factors for Pile Group Analysis. *23*(4), s. 441-450.

Ern, A., & Guermond, J. (2004). *Theory and Practise of Finite Elements.* New York: Springer-Verlag.

Fleming, K., Weltman, A., & Randolph, M. (2009). *Piling Engineering.* New York: Taylor & Francis.

Gąsiorowski , D. (2022). Impact of the Finite Element Mesh Structure on the Solution Accuracy of a Two-Dimensional Kinematic Wave Equation. *Water*, s. 446.

Guo, W. D. (2012). *Theory and practice of pile foundations.* FL, USA: CRC Press.

Hirai, H. (2012, December 10). A Winkler model approach for vertically and laterally loaded piles in nonhomogeneous soil. *Numerical and Analytical Methods in Geomechanics*, s. 1869-1897.

İşbuğa, V. (2023). An Interaction Model Between Two Vertically Loaded Piles. *(Submitted)*.

Kitiyodum, P., Matsumoto, T., & Sonoda, R. (2011). Approximate Numerical Analysis of a Large Piled Raft Foundations. *Soils and Foundations, 51*(1), s. 1-10.

Kong, Q., Siauw, T., & Bayen, A. (2020). *Python Programming and Numerical Methods.* Academic Press.

Liang, F., & Zong, Z. (2014). BEM Analysis of the Interaction Factor for Vertically Loaded Dissimilar Piles in Saturated Poroelastic Soil. *Computers and Geotechnics*(62), s. 223-231.

Logan, D. L. (1986). *A First Course of Finite Element Method.* Boston: PWS Engineering.

Mandolini, A., & Viggani, C. (1997). Settlement of Pile Foundations. *Géotechnique, 47*(4), s. 791-816.

Muki, R., & Sternberg, E. (1970). Elastostatic load-transfer to a half-space from a partially embedded axially loaded rod. *International Journal of Solids and Structures, 6*(1), s. 69-90.

Mylonakis, G., & Gazetas, G. (1998). Settlement and additional internal forces of grouped piles in layered soil. *Géotechnique, 48*(1), s. 55-72.

Pincus, H. J. (2003). Rock Mechanics. R. A. Meyers içinde, *Encyclopedia of Physical Science and Technology* (Third Edition b., s. 357-379). New York: Academic Press.

Polo, J. M., & Clemente, J. L. (1988). Pile-Group Settlement Using Independent Shaft and Point Loads. *Journal of Geotechnical Engineering, 114*(4), s. 469-487.

Poulos, H. G. (1968). Analysis of the Settlement of Pile Groups. *Géotechnique, 18*(4), s. 449-471.

Poulos, H. G., & Davis, E. H. (1980). *Pile Foundation Analysis and Design.* Wiley.

Randolph, M. F., & Wroth, C. P. (1978, December 1). Analysis of Deformation of Vertically Loaded Piles. *Journal of the Geotechnical Engineering Division, 12*(104), s. 1465-1488.

Randolph, M. F., & Wroth, C. P. (1979, December). An Analysis of the Vertical Deformation of Pile Groups. *Geotechnique*(29), s. 423-439.

Reddy, J. N. (2005). *An Introduction to Finite Element Method* (3. Edition b.). New York: McGraw-Hill.

Reese, L. C. (1964). Load versus Settlement for an Axially Loaded Piles. *Proceedings. Symposium on Bearing Capacity.* Roorkee: Central Building Research Institute,.

Salgado, R. (2008). *The Engineering of Foundations.* New York: McGraw Hill.

Scott, R. F. (1981). *Foundation Analysis.* NJ: Prentice Hall.

Seed, H. B., & Reese, L. C. (1957). The Action of Soft Clay along Friction Piles. *Transactions of the American Society of Civil Engineers, 122*(1), s. 731-754.

Simulia. (2008). *Getting Started with Abaqus.* USA: Dassault Systemes.

Teodoru, & Bogdan, I. (2009). Beams on elastic foundation the simplified continuum approach. *Buletinul Institutului Politehnic din lasi. Sectia Constructii, Arhitectura, 55*(4), s. 37.

Thote, N. R., Wajid, S., & Saharan, M. (2016, 01). Effect of shape of opening on the stability of caverns: an experimental analysis.

Vallabhan, C. V. (1994). Validity of the Reese model for pile foundations using energy principles. *Texas ASCE Conference.* Texas.

Vallabhan, G. C., & Mustafa, G. (1996). A New Model for the Analysis of Settlement of Drilled Piers. *International Journal for Numerical and Analytical Methods in Geomechanics, 20*, s. 143-152.

Vallabhan, G. C., Straughan, T. W., & Das, Y. C. (1991). Refined model for analysis of plates on elastic foundations. *Journal of engineering mechanics, 117*(12), s. 2830-2843.

Winkler, E. (1867). Die Lehre von Elastizitat und Festigkeit (on Elasticity and Fixity). *Dominicus*.

Wong, S. C., & Poulos, H. G. (2005). Approximate pile-to-pile interaction factors between two dissimilar piles. *Computers and Geotechnics, 32*(8), s. 613-618.

Zafarparandeh, I., & Lazoglu, I. (2012). Application of the finite element method in spinal implant design and manufacture. P. J. Davim içinde, *The Design and Manufacture of Medical Devices* (s. 153-183). Woodhead Publishing.

Zhou, P. (1993). *Numerical Analysis of Electromagnetic Fields.* Berlin, Heidelberg: Springer Berlin Heidelberg.